Fall 2021

# Investigation of anomalous data trends during coal dust explosibilty testing

Jacob Lee Miller

# INVESTIGATION OF ANOMALOUS DATA TRENDS DURING COAL DUST EXPLOSIBILTY TESTING

by

JACOB LEE MILLER

A DISSERTATION

Presented to the Graduate Faculty of the

MISSOURI UNIVERSITY OF SCIENCE AND TECHNOLOGY

In Partial Fulfillment of the Requirements for the Degree

DOCTOR OF PHILOSOPHY

in

EXPLOSIVES ENGINEERING

2021

Approved by:

Catherine Johnson, Advisor
Paul Worsey
Grzegorz Galecki
Kyle Perry
Frank Liou

## ABSTRACT

Coal dust explosibility is a health and safety concern that has been a recognized hazard for over 100 years. Initial testing by the Author using a Siwek 20L apparatus recorded a secondary maximum pressure at higher dust concentrations (1,000-7,000g/$m^3$) with Pulverized Pittsburgh Coal (PCC). Higher dust concentrations are beyond the typical ASTM E1226 testing procedure but are possible in mining and processing scenarios. No reference documents have been discovered that show a secondary maximum pressure at higher dust concentrations. Literature reviewed identified that once a coal dust concertation generates a peak pressure, the pressure remains constant or decreases only slightly with continuously increasing coal dust concentrations.

The primary goal of this research is to investigate the source of a secondary peak pressure for higher concentrations of PPC dust. Testing presented within this dissertation has shown that the maximum explosion pressure does not behave in a linear fashion as concentration levels increase.

The Author's proposed theory is the particle size distribution in a given sample, at higher concentrations, is undergoing secondary comminution and air classification during injection that leads to an enrichment of fines being tested. The dust being combusted during the explosive testing is not the same dust loaded into the test apparatus. The dust being evaluated within the combustion chamber possesses a higher quantity of fine PPC dust and has less mass than the sample loaded. To date, the Author has tested PPC dust concentrations ranging from 30 to 3,000 g/$m^3$. To test the Authors theory four objectives were identified and evaluated.

# ACKNOWLEDGMENTS

A special thanks to my Wife and children. I've been going to college for 24 years. I know it has been bothersome and inconvenient at times. Your patience with my physical and mental absence is greatly appreciated. I fondly remember the times each of you has helped me conduct research, sometimes late into the night...for months at a time.

# TABLE OF CONTENTS

Page

## LIST OF ILLUSTRATIONS

Page

# LIST OF TABLES

# NOMENCLATURE

| Symbol | Description |
|---|---|
| 20L | 20 liters |
| ASTM | American Society for Testing and Materials |
| cal | calorie |
| $C_L$ | Lowest quantity of fuel that allows for combustion |
| $C_{peak}$ | Quantity of fuel that produces the highest combustion pressure |
| Cstoich | The theoretical quantity of fuel that complete and balanced combustion reaction will occur. |
| $C_U$ | Highest quantity of fuel that allows for combustion |
| D10 | A diameter at which 10 percent of a sample's mass is comprised of particles with a diameter less than the reported value. |
| D50 | A diameter at which 50 percent of a sample's mass is comprised of particles with a diameter less than the reported value. (median) |
| D90 | A diameter at which 90 percent of a sample's mass is comprised of particles with a diameter less than the reported value. |
| D(3,2) | The particle size with the mean surface area of an analyzed sample. |
| $(dP/dt)_{ex}$ | Maximum rate of the pressure increase per unit time during a single deflagration test. (bar/s) |
| $(dP/dt)_{max}$ | Maximum value for the rate of pressure increase per unit time reached during the complete course of deflagration tests. (bar/s) |
| g | gram |
| $g/m^3$ | gram per meter cubed |
| kJ | kilojoule |
| Kst | The deflagration index. A parameter to designate explosive severity. (bar*m/s) |

| | |
|---|---|
| $(Kst)_{max}$ | Maximum deflagration index during the complete course of a deflagration tests. (bar*m/s) |
| ms | millisecond |
| NFPA | The National Fire Protection Association |
| NIOSH | The National Institute for Occupational Safety and Health |
| OSHA | The Occupational Safety and Health Administration |
| PPC | Pulverized Pittsburgh Coal |
| PRL | Pittsburgh Research Laboratory |
| $P_{ex}$ | Maximum explosion pressure during a single deflagration test. (bar) |
| $P_{max}$ | Maximum explosion pressure produced during the complete course of deflagration tests. (bar) |
| s | second |
| SkG | Skewness - a mathematical expression that describes the preferential spread of particle size distribution away from the average |
| USBM | United States Bureau of Mines |

# 1. INTRODUCTION

Coal dust explosibility is a problem within the coal mining and succeeding use in industry such as bulk commodity shipping and powerplant stockpiling. Though recognized as a hazard over 100 years ago, coal dust explosions claim lives and destroy mines up to present day. The literature reviewed for this effort has primarily identified that once a coal dust concertation generates a peak pressure, the pressure remains constant or decreases slightly with continuously increasing coal dust concentrations. To date, no reference data has been found that presents a secondary maximum pressure at higher dust concentrations (1,000-7,000g/$m^3$). However, preliminary testing has indicated that the maximum pressure does not behave in a linear fashion as concentration levels increase. The information presented in this dissertation will assist in the understanding the effects of coal dust explosions across all concentrations.

The primary goal of this research is to investigate the source of a secondary peak pressure for higher concentrations of Pulverized Pittsburg Coal (PPC) dust. The literature review lead to the identification of three key variables for examining the characteristics of coal dust explosions. These variables are the concentration of dust in the air, the particle size of the dust, and the distribution of dust particle sizes.

The hypothesis is particle size distribution in a given sample, at higher concentrations, is undergoing secondary comminution and air classification during injection into a Siwek 20L vessel that leads to an enrichment of fines being tested. The PPC will be examined per the explosive dust characteristics set forth by the ASTM E1226, Standard Test Method for Pressure and Rate of Pressure Rise for Combustible

Dusts. The explosibility characteristics defined by ASTM E1226 include: maximum explosion pressure, ($P_{max}$); maximum rate of pressure rise, $(dP/dt)_{max}$; and explosibility index, ($K_{st}$). To date, the student has tested PPC dust concentrations ranging from 30 to 3000 g/m$^3$. To achieve the goal of the proposed research, the following four objectives have been identified to test the hypothesis.

Table 1-1. Review of Objectives

| | **Objectives** |
|---|---|
| 1 | Identify Peak Pressure and dust concentration that creates peak pressure between 250 and 500 g/m$^3$. |
| 2 | Quantify dust particle size and distribution that is injected into the combustion chamber. |
| 3 | Quantify dust mass, particle size and distribution that is not injected into the combustion chamber and stays behind in loading chamber. |
| 4 | Identify if tight particle distribution correlates to explosion peak pressure and pressure trends vs high dust concentrations. |

The standard testing increments leave a range of concentrations unevaluated. The rise in the $P_m$ between dust concentrations of 200 and 500 g/m$^3$ is relatively constant. Beyond the dust concentration of 500 g/m$^3$ it can be seen that $P_m$ corrected trends downward. For Objective 1 the hypothesis is a higher $P_{max}$ exists between the initial dust concentrations evaluated by the author. A more well-defined $P_{max}$ value is needed to compare higher dust concentrations reaction pressures with more precision.

The operation procedure of the Siwek 20L apparatus has an unwritten assumption that the dust loaded within the loading chamber is the same size and particle distribution of the dust injected into the combustion chamber. Objective 2 tests the hypothesis that all the dust particle size and distribution of dust injected is different than the feedstock's characteristics.

A second assumption is all of the dust in the loading chamber is injected into the combustion chamber. Objective 3 will show if air classification is occurring during dust injection and distribution thus shifting the dust size distribution. It is hypothesized that larger particles are not injected consistently because they are more prone to fall out of suspension when air flows from the loading chamber to the explosive testing chamber.

Objective 4 will test the hypothesis that a narrow dust size distribution will decrease test output variability. The author speculates that a narrow dust size distribution will not generate the second peak pressure at high concentration levels as seen with the as received PPC feedstock.

The research provides a significant contribution to the industry by expanding the current theory of coal dust explosibility to include the influence dust particle size distribution has on peak pressure at higher concentrations. The data collected throughout this research has been utilized to publish two journal papers and one conference proceeding. The focus of the published papers have been: 1) a review of historic published data compared to tests conducted by the student following ASTM E1226 [1], 2) a complete detailed analysis of PPC dust at low concentrations per ASTM E1226 [2], and 3) an extended analysis of PPC dust particle size distribution for concentrations greater than 1,000 g/m$^3$ [3]. Data yet to be published relates to: the mass and particle size distribution of PPC dust injected into the test chamber and dust not injected into the test chamber, the effects of tight particle distribution on explosion peak pressure vs dust concentrations for concentrations greater than 1000 g/m$^3$.

# 2. LITERATURE REVIEW

The literature review covers several topics to build supporting information related to dust explosions, specifically coal dust explosions. The review starts with a brief review of the recorded history of major coal dust explosions and then transitions into examining properties that influence dust explosions. Next the literature review presents several published papers that cover explosive characteristics of coal dusts tests conducted at low and high levels of dust concentration. Finally, the current ASTM testing standard E1226 is reviewed and subsequently compared to testing conducted by the USBM before ASTM testing standards were created. The literature review is laid out to establish the danger that coal dust explosions present to industry, what characteristics influence the dust explosion, what testing has been done in the past, and how the testing in the past differs from current testing standard procedures.

## 2.1. INTRODUCTION INTO COAL DUST EXPLOSIONS

In the United States, coal dust explosions have historically exceeded 500 deaths per year with some incidents claiming 200 or more lives [4]. Since 2001, fatal coal mine explosions include; No. 5 Mine (13 killed, 2001), Sago Mine (12 killed, 2006), Darby Mine No. 1 (5 killed, 2006), and Upper Big Branch Mine (29 killed, 2010) [5].

For a dust explosion to occur, several conditions must be met [6]. The dust must be: combustible, suspended in an atmosphere capable to support flame, have a particle size distribution capable of propagating flame, at a concentration that is within its explosibility range, and be exposed to an ignition source of sufficient energy to initiate combustion. OSHA asserts that five factors must be present simultaneously for a combustible dust explosion to occur. The factors are Fuel, Oxygen, Heat, Dispersion, and Confinement [7]. The five factors are illustrated in Figure 2-1 as the Explosion Pentagon.


Figure 2-1. Explosion Pentagon [7]

Coal dust and its ability to explode when distributed into the air has been a topic of concern for over 200 years [8]. As coal became the power source for the industrial revolution in the early 1700s, the demand and use of coal grew exponentially. By the early, to mid-1800’s it was theorized that coal dust could cause or enhance a coal mine explosion. The Prussian Fire-Damp Commission in 1884, the Commission on Explosions in Mining in 1891, The Royal Commission in 1894, among others, conducted some of the earliest identified research on explosibility of coal dust. By the early 1900s, the English Royal Commission and Taffanel of France had concluded that coal dust could support an explosion without the support of Methane [9].

The United States Congress appropriated funds for the Federal Geological Survey to begin an investigation of mine explosions in 1907 after a series of eighteen-coal mine disasters occurred in the United States within a year. The worst two disasters in 1907 occurred within two weeks of each other in December at Monongah and Darr Mines, killing over 600 people [4]. By 1910, the United States Bureau of Mines (USBM) was created and tasked with continuing the mine explosion research. In addition to full-scale testing, the USBM developed new methods of testing coal dust explosibility in a laboratory setting. These included the Pittsburgh Research Laboratory 20-Liter test vessel (PRL 20L), a 1-$m^3$ chamber, and the 1.2-liter vessel known as the Hartmann tube apparatus. The USBM quantified coal dust explosibility as a function of the maximum explosion pressure ($P_{max}$), the maximum rate of pressure rise $(dP/dt)_{max}$, and explosibility index ($K_{st}$), collected from years of research with Pulverized Pittsburg Coal (PPC) [10] [11] [12]. The USBM was disbanded in 1996 by the United States Conrgress and President Bill Clinton because of waning public support and decreased political clout [10].

The American Society for Testing and Materials (ASTM) was founded in 1898. The organization dedicated itself to “the development and unification of standard methods of testing; the examination of technically important properties of materials of construction and other materials of practical value, and also to the perfection of apparatus used for this purpose. [13]” In 2000, ASTM developed test method ASTM E1226 to provide a standard test method to characterize the “explosibility” of particulate solids of combustible materials suspended in air [14].

A materials' explosibility is characteriazed with quanantative data with variables denoted as $P_{max}$, $(dP/dt)_{max}$, and $K_{st}$ values. Cashdollar in 1985 published that the USBM utilized these variables for the evaluation of coal dust. These same variables are utilized by ASTM for similar purposes in ASTM E1226. The data provided by the USBM was generated before the creation of ASTM E1226. To the student's knowledge no widely published evaluation on PPC dust has been conducted following ASTM E1226. The student conducted such an evaluation in the preliminary work for this research and subsequently published [2]. The current ASTM test standard may influence the dust explosion characteristic parameters $P_{max}$, $(dP/dt)_{max}$ and $K_{st}$.

## 2.2. PROPERTIES THAT INFLUENCE DUST EXPLOSIBILITY

Physical properties of dust and their clouds affect the explosibility and explosion magnitude of an explosive dust reaction event. Echoff discusses how particle size, dust concentration, and turbulence affect the characteristics of a dust explosion [6]. The influence of the properties are summarized in Table 2-1.

Table 2-1. Dust Properties and Their Effect on Explosibility Characteristics when Properties are Increased [6]

| | |
|---|---|
| Particle Size | Decreases $P_{max}$, $(dP/dt)_{max}$, and $K_{st}$ |
| Dust Concentration | Increases $P_{max}$, $(dP/dt)_{max}$, and $K_{st}$ until peak pressure is reached then Decrease |
| Turbulence | Increases $P_{max}$, $(dP/dt)_{max}$, and $K_{st}$ |
| Moisture | Decreases $P_{max}$, $(dP/dt)_{max}$, and $K_{st}$ |
| Initiation Pressure | Increases $P_{max}$, $(dP/dt)_{max}$, and $K_{st}$ |
| Initiation Energy | Increases $P_{max}$, $(dP/dt)_{max}$, and $K_{st}$ |

The dust properties have a potential influence on dust explosibility and are of critical importance to this research. A more detailed discussion of each dust property is discussed in the following subsections.

**2.2.1. Particle Size.** The particle size distribution of a powder controls whether a combustible dust can support an explosion. An average particle diameter of 500 micron is often regarded as the maximum size particle that can support an explosion [15]. In Figure 2-2, the particle size distribution can be seen affecting the severity of dust explosions.

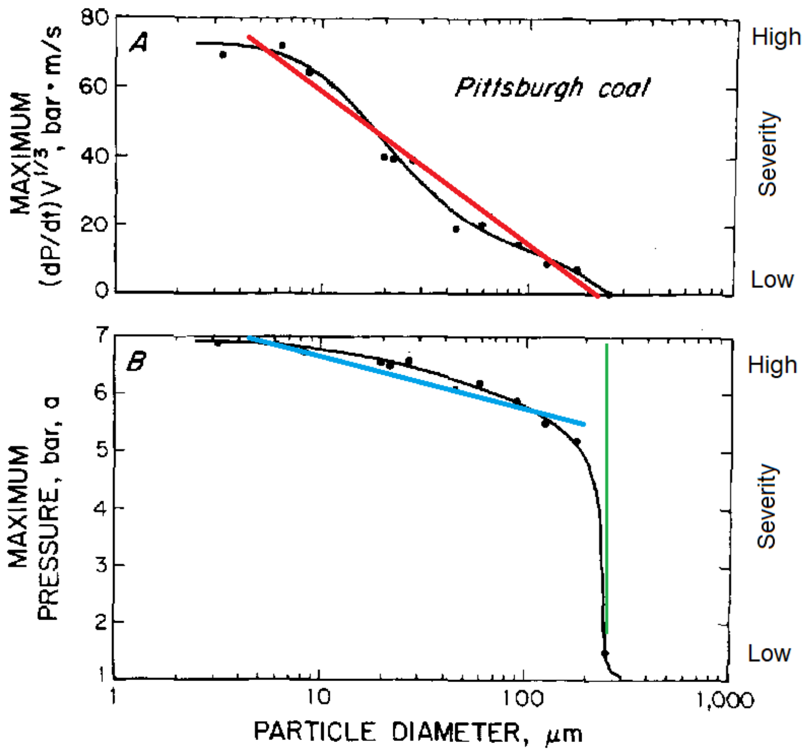


Figure 2-2. Effect of Dust Size on Explosibility Characteristics. A Plots $K_{st}$ and B Plots $P_{max}$ vs Coal Dust Particle Size, Modified from [16]

Large particles have a relatively small specific surface area and explode with less energy, characterized with lower measured values of $K_{st}$ and $P_{max}$   Small particles have a high specific surface area and exhibit higher $K_{st}$ and $P_{max}$ values [16]. In Figure 2-2A the change in $K_{st}$ is roughly linear as dust particle size increases on a log scale. The trend is depicted with a red line showing decreased rate of reaction as particle size increases. The logarithmic relationship denotes that $K_{st}$ is heavily dependent on particle size.

The slight change in $P_{max}$, shown in Figure 2-2B and denoted by a blue line, denotes a low sensitivity to particle size until a limit is reached. Once the limit is reached, the trend becomes asymptotic (depicted by a green line). The particle size has increased over almost 2 magnitudes from approximately 2 microns to 200 microns while the $P_{max}$ only decreased about 20 percent. Above a critical particle size combustion does not propagate effectively and no explosion occurs. $P_{max}$ is predominantly driven by the chemical nature of the material undergoing combustion during a dust explosion rather than particle size [6].

**2.2.2. Concentration.** The concentration of the dust particles has a direct effect on the behavior of dust explosions. In Figure 2-3 an ideal dust concentration, fuel, vs peak explosion presssure  can be observed with three regions: lean, optimum and rich [6]. A lean condition is when there is a scarcity of fuel and this region is bound by $C_L$ to $C_{stoich}$.

The optimum region is between the stoichiometric ratio $C_{stoich}$ and $C_{peak}$ where a maximum value is reached in explosion severity, $K_{st}$ and explosion pressure, $P_{max}$. Any further increase beyond $C_{peak}$ in concentration results in a decrease in both $K_{st}$ and $P_{max}$.

The decrease is a result of the excess powder absorbing some of the energy released during combustion and insufficient oxygen to react with the excess powder. The rich region is bound by $C_{peak}$ and $C_U$.

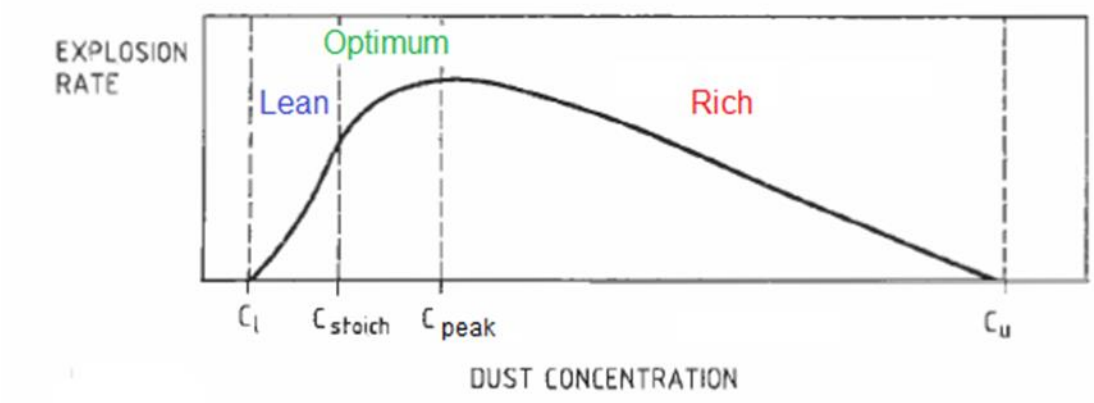


Figure 2-3. Ideal Dust Concentration vs Rate of Explosive Dust Reaction, Adapted from [6]

**2.2.3. Moisture.** Moisture in the dust reduces the ignition sensitivity and explosion maximum rate of pressure change, $(dP/dt)_{ex}$ ,of dust clouds. Figure 2-4 shows how the explosion's $(dP/dt)_{ex}$ steadily reduces with increasing dust moisture content.

Moisture reduces the explosive characteristics of a dust explosion in several ways. 1) The heating and evaporating of water consumes heat so it is not available to propagate combustion; 2) The mixing of water vapor with pyrolysis gases prior to entering a combustion zone displaces oxygen and subsequently makes the combustion less reactive and 3) Moisture increases inter-particle cohesion of the dust thus preventing dispersion and increasing effective particle size of dust dispersed [6].

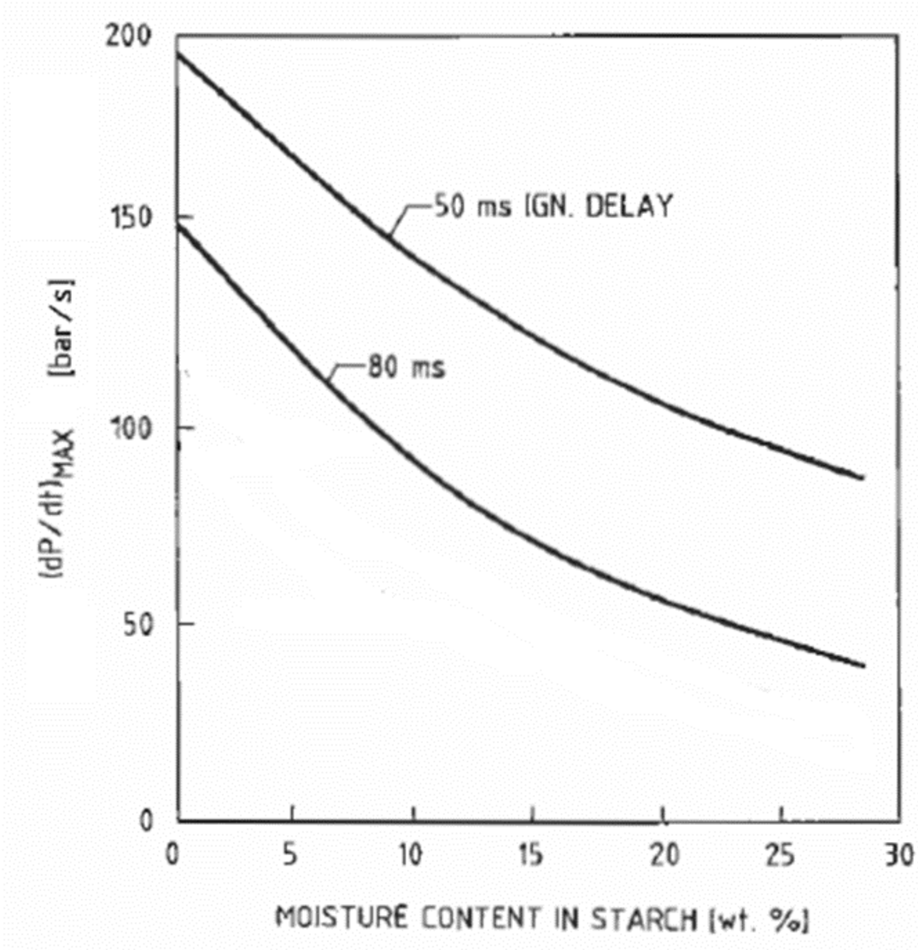


Figure 2-4. Influence of Moisture in Starch on Maximum Rate of Pressure Rise, Modified from [6]

**2.2.4. Ambient Pressure.** The ambient pressure in which the dust cloud is ignited within influences the dust explosion characteristics. The maximum explosion pressure increases with an increase in ambient pressure [6]. Figure 2-5 depicts the influence of initial ambient pressure on the maximum explosion pressure. Maximum explosive pressure increases as the ambient pressure of the test vessel increases.

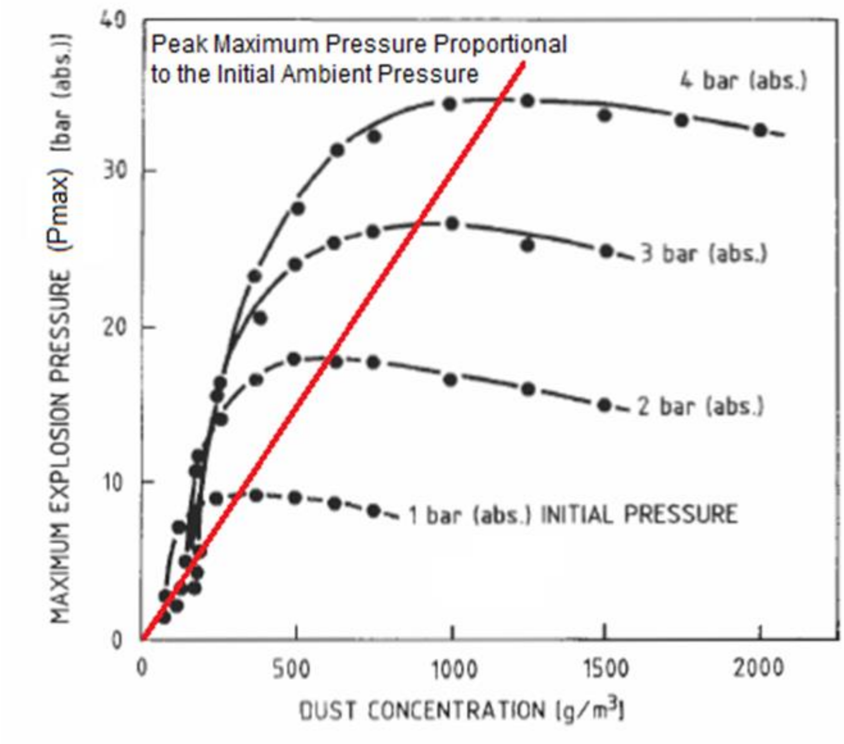


Figure 2-5. Maximum Explosion Pressure vs Dust Concentrations for Different Ambient Pressures, Modified from [6]

It is noted by Echoff  that, “the peak maximum pressure is proportional to the initial ambient pressure, as indicated by the straight line.” [6]  The plot of the straight red line in Figure 2-5 depicts the most efficient combustion at a given ratio of dust mass to air mass and represents the maximum peak pressure relative to the initial ambient pressure.  This optimum mass ratio is independent of initial ambient pressure.

**2.2.5. Ignition Energy.** Ignition energy also effects dust explosion characteristics. As ignition energy increases the $P_{max}$, $(dP/dt)_{max}$, and $K_{st}$ increase when compared to the same dust concentration evaluated with a lower ignition energy.  In Figure 2-6 the $P_{max}$ and $K_{st}$ of an explosive dust are plotted vs different dust concentrations.  Two different ignition energies were used, 2.5 kJ and 10 kJ, which have trend lines plotted black and red respectively. The 10 kJ ignition data results in higher $P_{max}$ and $K_{st}$ values than the 2.5 kJ ignition data for the same dust concentrations value. The dust explosion characteristics also increase faster and have a steeper trend line slope, for the 10 kJ data compared to the 2.5 kJ data. This indicates a strong relationship between dust explosion characteristics and ignition energy.

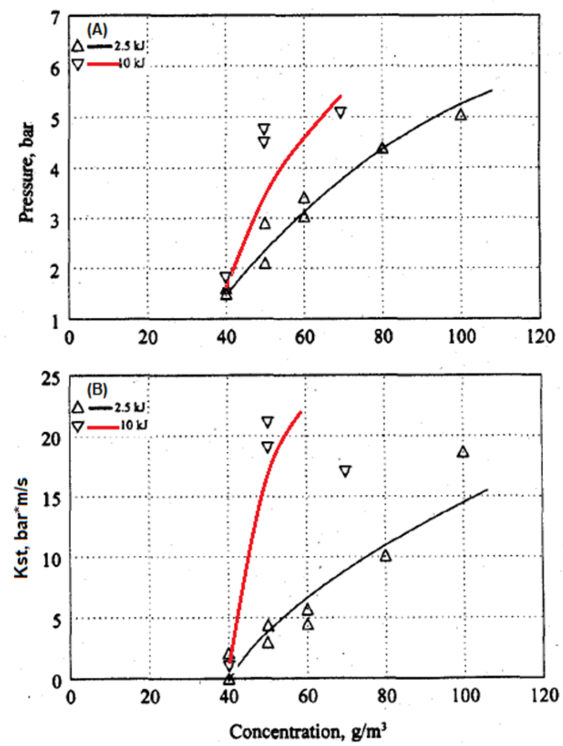


Figure 2-6. Dust Explosion Characteristics vs Dust Concentrations, Modified from [17]

**2.2.6. Turbulence.** Turbulence in dust explosions is the rapid movement of dust particles relative to each other. Turbulence gives rise to the mixing of oxygen, hot gases, burning particles and unburned particles. Higher turbulence results in a faster mixing of all the constituents within the dust explosion allowing the reaction to happen faster. This effect can be seen in Figure 2-7. Echoff observed that turbulence in the chamber decreased with time after dispersion and the initiation times were delayed correlating to different levels of turbulence [6]. Figure 2-7 highlights the influence of initial turbulence on explosive dust characteristics $P_{max}$ (Figure 2-7A) and $K_{st}$ (Figure 2-7B).

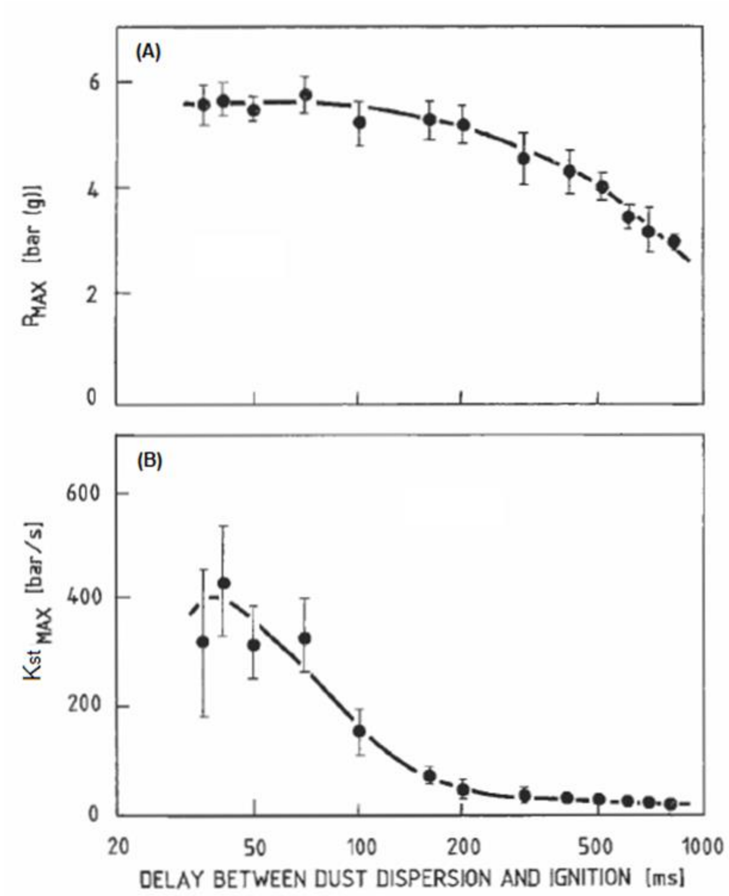


Figure 2-7. Initial Turbulence Effect on Explosive Dust Characteristics. A is $P_{max}$ and B is $K_{st}$, Both Plotted in Relation to Dust Dispersion Delay in ms. Modified from [6]

Initial turbulence is the turbulence generated by a short blast of air dispersing dust within a closed vessel. As time increases from the initial blast of air the dust particles slow down and stops mixing. The $P_{max}$ (Figure 2-7A) does not change initially, but, after

100 milliseconds it decreases slightly. $P_{max}$ reaches half its peak value when the turbulence has subsided. The $K_{st}$ (Figure 2-7B) decreases rapidly with a decrease in turbulence. At 100 milliseconds the $K_{st}$ is less than half its peak value and in another 100 milliseconds is an order of magnitude lower that its peak value.

## 2.3. LOW CONCENTRATION DUST TESTING (40-1,000 g/m$^3$)

Coal dust testing is typically conducted in the 40-1000 g/m$^3$ range. The USBM was a major source of research into coal dust explosions until its closure in 1995 [10]. The USBM data on coal dust explosibility has been the primary reference for research into coal dust since its founding in 1911 [9]. Cashdollar first published coal dust explosion data produced in a 20 Liter vessel in 1985 [18].

**2.3.1. United States Bureau of Mines Coal Dust Test.** In the 1980's the USBM conducted a series of coal dust explosion tests utilizing their internally designed PRL 20L chamber. The USBM used pulverized coal dust from a Pittsburgh coal seam. Pittsburgh coal is a name given to a thick, continuous and wide spread coal bed located in Pennsylvania, West Virginia, Ohio, and Maryland covering an area over 13,000 km$^2$ (5,000 mi$^2$) [19].

Table 2-2. Proximate Analyses of Pittsburgh Coal [16]

| | |
|---|---|
| Moisture (%) | 1 |
| Volatility (%) | 37 |
| Fixed Carbon (%) | 56 |
| Ash (%) | 6 |
| Heating Value (cal/g) | 7720 |

The standard PPC dust used by the USBM was described as being 80% minus 200 mesh (<75 µm), 13% minus 20 µm and a median particle diameter of 48 µm [16]. The proximate analyses of Pittsburgh coal is summarized in Table 2-2.

Cashdollar et.al. conducted tests at an ignition pressure of 1-atm by using pyrotechnic igniters of 2.5 kJ to initiate the coal dust explosions [18] [20]. The peak dust characteristic values reported are listed in Table 2-3.

Table 2-3. US Bureau of Mines Dust Explosion Characteristics for PPC, [18]

| | |
|---|---|
| $P_{max}$ | 6.9 bar |
| $(K_{st})_{max}$ | 36 bar*m/s. |

Figure 2-8a shows increasing $K_{st}$ values as dust concentration is increased from approximately 300 to 500 g/m$^3$. As the dust concentration increases, the variability of $K_{st}$ appears to increase and a trend is hard to discern. Figure 2-8b is a plot of the peak pressure measured at different dust concentrations showing that as the concentration increases the $P_{max}$ values increase. In Figure 2-4b, the pressure ratio increases rapidly to approximately 6.5 bar between dust concentrations of 0-300 g/m$^3$. However, around 300 g/m$^3$ the trend changes and the pressure remains relatively constant as dust concentration increases further.

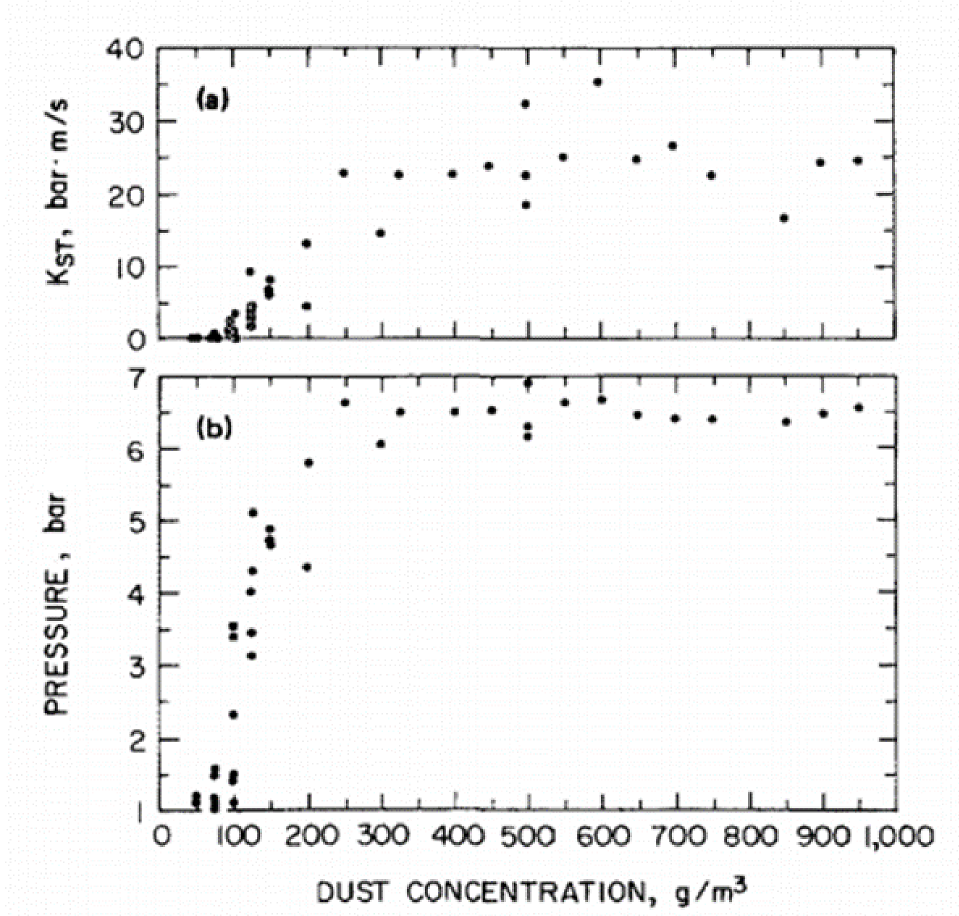


Figure 2-8. Explosibility Data for Pittsburgh Seam Coal Dust, Modified from [18]

**2.3.2. National Institute for Occupational Safety and Health Test.** The National Institute for Occupational Safety and Health (NIOSH) in 2014 tested the effect of coal dust particle size on the maximum explosion pressure, $P_{max}$. Dust was tested over a short range of concentrations from 60 g/m$^3$ up to 600 g/m3. Testing was conducted within a 1 m$^3$ chamber located at a Fike test facility [21]. Coal dust was listed as 20-60 mesh, course, medium, and pulverized Pittsburgh coal. The proximate analysis of the dust can be seen below in Table 2-4.

Table 2-4. Proximate Analysis for PPC per NIOSH, [21]

| Particle size (μm) | Coarse Pittsburgh coal, wt% | Medium Pittsburgh coal, wt% | Pulverized Pittsburgh coal, wt% |
|---|---|---|---|
| 212–850 | 57.2 | 28.8 | 0.2 |
| 150–212 | 9.0 | 7.7 | 0.8 |
| 106–150 | 8.2 | 10.7 | 5.9 |
| 75–106 | 5.7 | 13.6 | 13.5 |
| 53–75 | 5.9 | 14.2 | 22.8 |
| 38–53 | 3.7 | 7.5 | 17.2 |
| <38 | 10.3 | 17.5 | 39.6 |

During testing, Man and Harris investigated three different ignition energies. PPC and medium coal dust utilized 5 kJ ignitors. The coarse coal dust used 10 kJ ignitors. Coal designated as 20-60 mesh was tested with 20 kJ ignitors. The explosion pressure vs coal dust concentration can be seen in Figure 2-9.

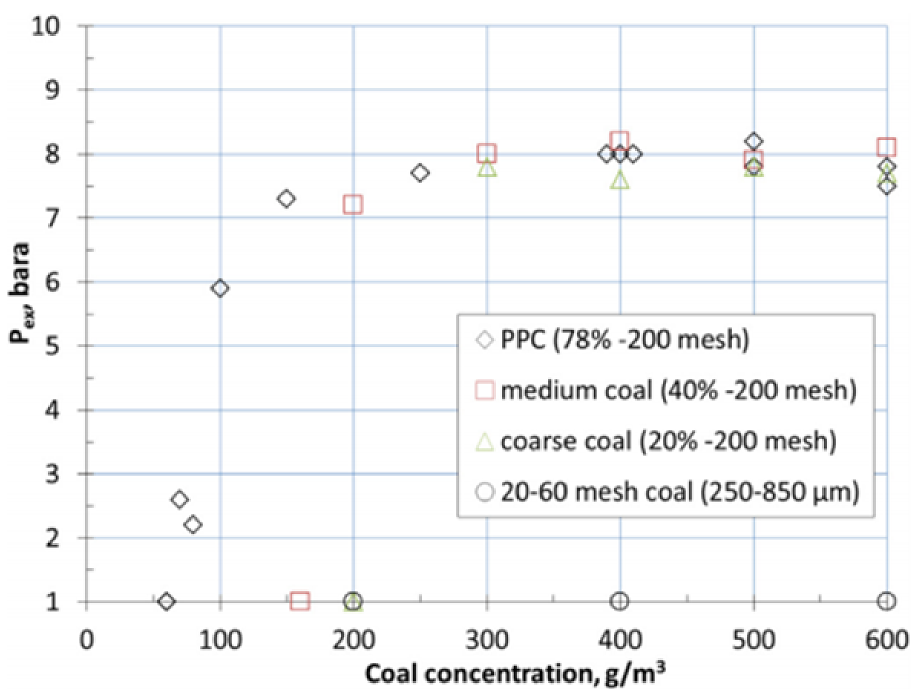


Figure 2-9. Effect of Coal Particle Size on Explosive Pressure, $P_{max}$, in a 1-m$^3$ Vessel [21]

The coarse, medium, and pulverized Pittsburgh coals each have similar $P_{max}$ values. The medium and course coal did not ignite initially at lower concentrations. Only when higher concentrations were tested did ignition occur in the medium and course coal. The largest coal dust particles, 20-60 mesh (841-250 microns) did not explode in the 1 $m^3$ chamber over the entire concentration range evaluated.

## 2.4. HIGH CONCENTRATION DUST TESTING (1,000-7,000 $g/m^3$)

Dust concentrations greater than 1000 $g/m^3$ exceed the specified testing requirements of ASTM E1226. However, high dust concentrations are possible in mines and processing plants. The explosive dust characteristics of coal at high concentrations is a viable concern and has been investigated by USBM [16]and agencies within other countries [22], [23].

**2.4.1. United States Bureau of Mines High Concentration Coal Dust Test**. Cashdollar expanded the USBM’s research on the explosibility of coal dust by examining the influence of coal volatility, particle size, oxygen concentrations, and amounts of limestone rock dust to inert the coal dust using the PRL 20L [16]. Cashdollar also expanded the coal dust concentration vs. explosion pressure curve to concentration levels of coal dust as seen Figure 2-10.

The extended explosibility data was conducted in a wider range of PPC dust concentrations. The highest concentration shown in Figure 2-10 was more than 4,000 $g/m^3$ while Figure 2-8 did not exceed a dust concentration of 1,000 $g/m^3$.

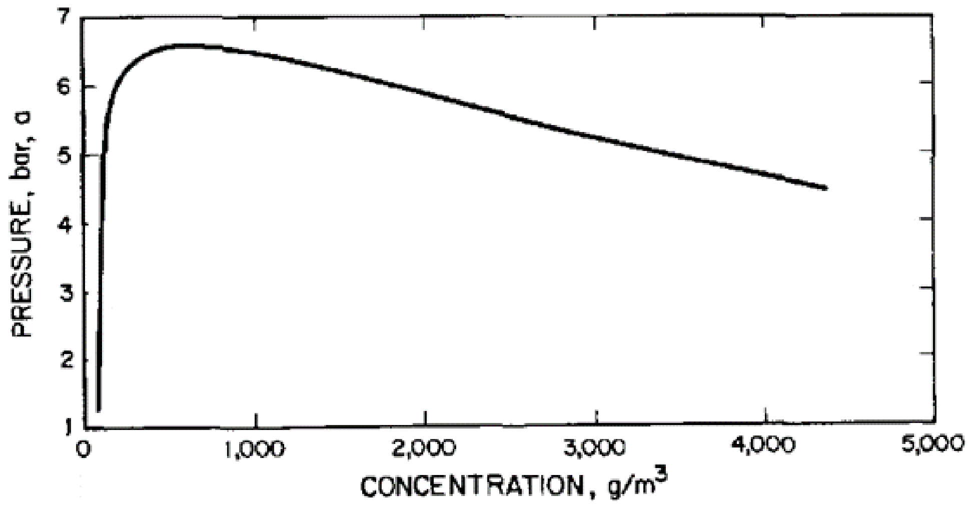


Figure 2-10. Expanded Explosibility Data for Pittsburgh Seam Coal Dust, modified from [16]

The plot in Figure 2-10 shows a rapid increase in pressure as the concentration increases and reaches a peak pressure around a dust concentration of 600 g/m$^3$. After the peak in pressure, the trend decreases in a linear fashion. The trend line in Figure 2-10 matches the data shown in Figure 2-8, well within the limits of dust concentrations shown in Figure 2-8.

**2.4.2. Explosibility of Victorian Brown Coal Dust.** In 1988 the findings from experiments conducted in Australia on Morwell coal were published by Woskoboenko [22]. The explosive dust characteristics, maximum explosion pressure, maximum rate of pressure rise and explosibility index where investigated. A wide range of dust concentrations from 150 g/m$^{3\ \mathrm{to}}$ 7,000 g/m$^3$ were evaluated. The median dust particle size was 22 microns. More information on the coal properties can be seen in Table 2-5. These values vary from the proximate analysis of PPC seen in Table 2-2 where PPC values are higher except for moisture and ash percentages.

Table 2-5. Proximate Analysis for Victorian Brown Coal, [22]

| | |
|---|---|
| Moisture (%) | 3.92 |
| Volatility (%) | 27.18 |
| Fixed Carbon (%) | 69.9 |
| Ash (%) | 2.8 |
| Heating Value (cal/g) | 6597 |

Testing was conducted with a 20-L Spherical Vessel similar to a Siwek 20L sphere. Two pyrotechnic initiators with a total energy of 10 kJ were used to ignite each test. The results of the investigation of coal dust explosion characteristics can be seen in Table 2-6 and Figure 2-11.

The maximum pressure ($P_{max}$) , $(dP/dt)_{max}$, and $(K_{st})$max values can be found in Table 2-6. The $P_{max}$ had a value of 7.6 bar. The maximum rate of pressure rise, Dp/dt, was 550 bar/s which results in a $(K_{st})_{max}$ of 220 bar*m/s.

Table 2-6. Dust Explosion Characteristics for Victorian Brown Coal, [22]

| | |
|---|---|
| $P_{max}$ | 7.6 bar |
| $(dP/dt)_{max}$ | 550 bar/s |
| $(K_{st})_{max}$ | 220 bar*m/s. |

In Figure 2-11, the complete data set of the explosive dust evaluation is plotted with a log scale along the dust concentration axis. Maximum pressure and maximum rate of pressure rise, $(dP/dt)_{max}$, attain peak values at a dust concentration of 500 g/m$^3$. All trend lines rise rapidly as dust concentration increases from the initial values of 150 g/m$^3$ up to the value of 500 g/m$^3$. After the dust concentration of 500 g/m$^3$, the trend lines show a slow decrease in recorded characteristic data until the maximum evaluated dust concentration of 7,000 g/m$^3$ is reached. The maximum rate of pressure rise, $(dP/dt)_{max}$, as well as the maximum pressure values show a continuous decline from dust concentrations of 500 g/m$^3$ to 2,000 g/m$^3$. Beyond the dust concentration of 2,000 g/m$^3$ there is no data except a dust concentration of 7,000 g/m$^3$. At a dust concentration of 7,000 g/m$^3$ no explosive reaction occurred.

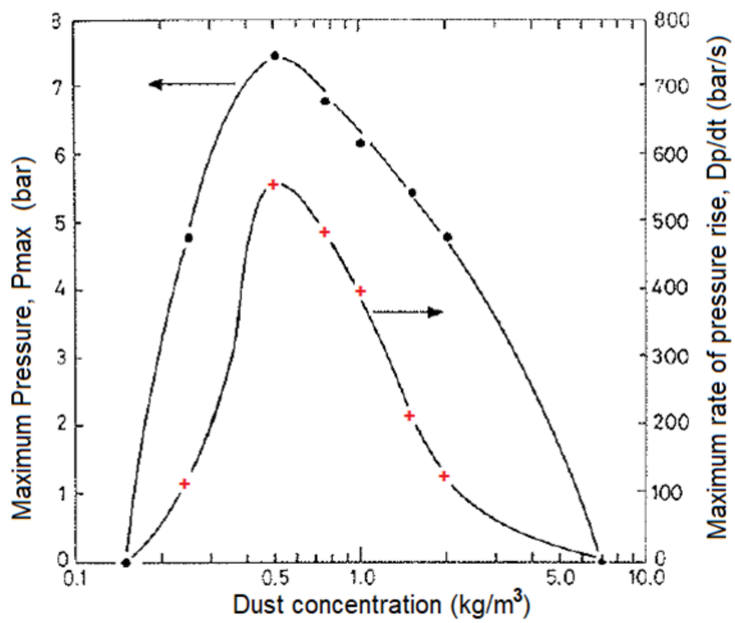


Figure 2-11. Maximum Pressure and Maximum Rate of Pressure Rise vs. Victorian Brown Coal Dust Concentrations, modified from [22]

**2.4.3. Study of Coal Dust Explosibility Data for Designing Explosive Safety Measures.** Dr. Mittal in 2013 published the findings from experiments conducted in India on coal sourced from the Jharia coalfields of India. This study investigated the explosive hazards of two indigenous coal dusts. Explosive dust characteristics, maximum explosion pressure, maximum rate of pressure rise and explosibility index were investigated. The determination of explosive dust characteristics was conducted over a wide range of dust concentration (80-4,500 g/m$^3$) for two types of coals (coal A and coal B). Coal A and coal B had volatile matter of 27.18% and 19.69% respectively. All coal used was representative of pulverized coal for boiler fuel with 90% passing through a 200 mesh sieve. More information on the coal properties can be seen in Table 2-7. These values vary from the proximate analysis of PPC seen in Table 2-2 where PPC values are higher except for moisture and ash percentages.

Table 2-7. Proximate Analysis for India Coal, [23]

| | Coal A | Coal B |
|---|---|---|
| Moisture (%) | 3.92 | 3.8 |
| Volatility (%) | 27.18 | 19.69 |
| Fixed Carbon (%) | 50.70 | 40.72 |
| Ash (%) | 18.20 | 35.79 |
| Heating Value (cal/g) | 6011.76 | 3684.91 |

Testing was conducted with a 20-L Spherical Vessel similar in design to the Siwek 20L sphere. Two pyrotechnic initiators with a total energy of 10 kJ were used to ignite each test evaluation of the dust. The results of the investigation of coal dust explosion characteristics can be seen in Table 2-8 and Figure 2-12.

Table 2-8 has the maximum pressure and $K_{st}$ values recorded during the investigation. Coal A has a higher $P_{max}$ and $(K_{st})_{max}$ than Coal B. The paper theorizes the higher dust explosion characteristics are due to the higher volatility, fixed carbon and heating value of Coal A. It should be noted that the explosive dust characteristic values for the coals in Table 2-8 are not very different even though the heating value of Coal B is only about 60 percent of Coal A.

Table 2-8. Dust Explosion Characteristics for India Coal, [23]

| | Coal A | Coal B |
|---|---|---|
| $P_{max}$ | 6.8 bar | 6.2 bar |
| $(K_{st})_{max}$ | 158 bar*m/s. | 140 bar*m/s. |

In Figure 2-12 the complete data set of the explosive dust evaluation can be seen for Coal A and Coal B. Both coals follow similar trends for $K_{st}$ and pressure and attain peak values at a dust concentration of 500 g/m$^3$. All trend lines rise rapidly as dust concentration increases from the initial values of 80 g/m$^3$ up to the value of 500 g/m$^3$.

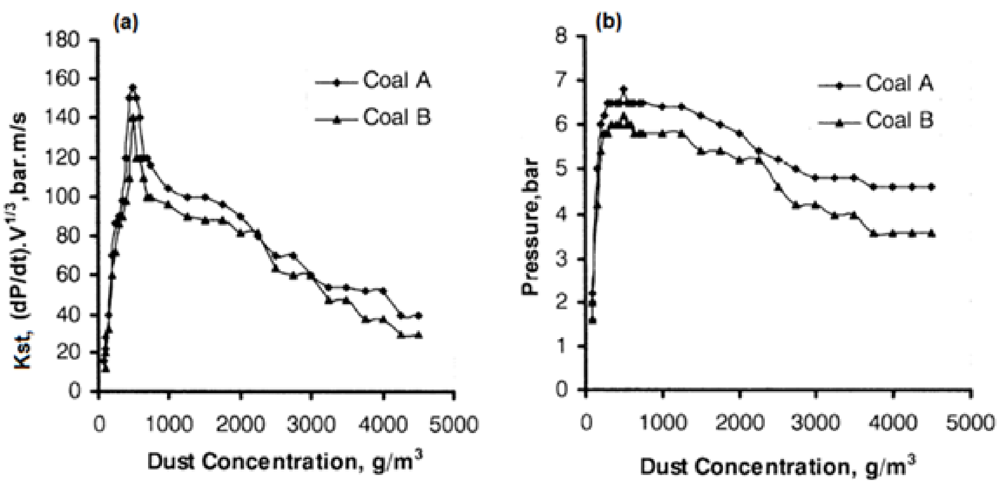


Figure 2-12. Explosibility Data for India Coal Dust, modified from [23]

After the dust concentration of 500 g/m$^3$ the trend lines show a slow decrease in recorded characteristic data until the maximum evaluated dust concentration of 4,500 g/m$^3$ is reached. $K_{st}$ values drop at a faster rate than the pressure values. $K_{st}$ values show a continuous decline from dust concentrations of 750 g/m$^3$ to 4,500 g/m$^3$. The published pressure data decreases slightly from dust concentrations of 750 g/m$^3$ to 4,500 g/m$^3$ but appears to no longer decrease with dust concentrations greater than 3,750 g/m$^3$.

## 2.5. ASTM STANDARD E1226

The purpose of the ASTM E1226 test method is to provide standard test methods for characterizing the explosibility of fine material evenly distributed in the air as a dust cloud. The test method is applied to all potentially flammable materials that are 420 microns or smaller in size. The standard first prescribes a procedure to determine if a dust is explosible with a screening test. If the dust is found to be explosible, then the severity of the explosibility is determined through a series of predetermined tests, which vary dust concentrations. Dust explosibility characteristics include:

- Maximum explosion pressure ($P_{ex}$): "The maximum pressure rise produced during a single deflagration test" [14].
- Maximum explosion pressure ($P_{max}$): "the maximum pressure rise produced during the complete course of deflagration tests" [14].
- Maximum rate of pressure rise $(dP/dt)_{ex}$: "the maximum rate of the pressure increase per unit time during a single deflagration test" [14].
- Maximum rate of pressure rise $(dP/dt)_{max}$: maximum value for the rate of pressure increase per unit time reached during the complete course of deflagration tests. [14].
- The deflagration index ($K_{st}$): a parameter to designate explosive severity. It is extensively used in the design for explosion vents and explosion suppression system. ($K_{st}$) is obtained using Equation 1:

$$K_{st} = (dP/dt) * V^{1/3,} \text{ where V is vessel volume in } m^3 \quad (1)$$

- Maximum deflagration index $(K_{st})_{max}$: Maximum $K_{st}$ calculated during the complete course of a deflagration tests.

ASTM E1226-12A is typcially conducted within 1m$^3$ test vessel or a smaller vessel like the Siwek 20L Sphere. Due to the volume and mass differences of the two different sized vessels, a mathematical formula is specified within ASTM 1226 to compensate for the cooling effect the walls of the Siwek 20L Sphere have on explosions. A mathematical correction ($P_m$) is performed on the measured $P_{ex}$, if the $P_{ex}$ value is greater than 5.50 bar. Equation 2 for the correction is taken from the Appendices of ASTM E1226-12A and is shown below.

$$P_m = 0.775\ P_{ex}^{1.15} \quad (2)$$

ASTM E1226-12A also covers the criteria for judging if the results are acceptable. The $P_{ex}$ for each dust concentration level has a mean value calculated. If the $P_{max}$ from any of the three test series deviates more than 5% from the mean of the three test series, then the dust evaluation at that concentration is suspected of being invalid. If the $(dP/dt)_{ex}$ and $K_{st}$ from one test series deviates more than 20% from the mean of the three test series then the dust evaluation at that concentration is suspected of being invalid. The maximum mean value of peak pressure, rate of pressure change and explosive index is reported at $P_{max}$, $(dP/dt)_{max}$; and $(K_{st})_{max}$.

ASTM E1226 is not used solely in the mining industry. The Occupational Safety and Health Administration (OSHA) was created by Congress to assure safe working conditions by setting and enforcing standards. These standards are mandatory and are applied to most businesses that have more than 10 employees. The Federal OSHA standards are known as 29 CFR Part 1910 and they address some aspects of explosive dust. To meet OSHA standards some of the National Fire Protection Association's (NFPA) codes and standards are incorporated into 29 CFR Part 1920 [24]. Explosive dust is regulated indirectly by OSHA through the Combustible Dust National Emphasis Program (NEP) and Compliance Directive CPL-03-00-008 [25]. The combination of the NEP and Compliance Directive empowers OSHA inspectors to evaluate and notify employers of failures to meet explosive dust requires [26].

The NFPA has codes and standards related to explosive dust that reference ASTM E1226 as a testing protocol [27]. The codes and standards include:

- NFPA 61, Standard for the Prevention of Fires and Dust Explosions in Agricultural and Food Processing Facilities
- NFPA 68, Standard on Explosion Protection by Deflagration Venting
- NFPA 69, Standard on Explosion Prevention Systems
- NFPA 484, Standard for Combustible Metals
- NFPA 654, Standard for the Prevention of Fire and Dust Explosions from the Manufacturing, Processing, and Handling of Combustible Particulate Solids
- NFPA 652, Standard on the Fundamentals of Combustible Dust
- NFPA 664, Standard for the Prevention of Fires and Explosions in Wood Processing and Woodworking Facilities

Industries that fall under OSHA and NFPA and process explosive dusts are varied. They include dusts composed of metals, wood, coal, plastic, bio-solids, flour, sugar and textiles [25].

**2.6. KEY DIFFERENCES BETWEEN USBM AND ASTM TESTS**

While the USBM and ASTM E1226-12A vessels are similar in volume there are some key differences between the tests that should be noted. The USBM vessel (PRL 20L) is not completely spherical and utilizes a different dust injection nozzle and methodology, see Figure 2-13. The PRL 20L vessel has the test material loaded at the base of the vessel within a distribution nozzle. The distribution nozzle has several orifices that disperse the dust in the chamber. The Siwek 20L Sphere is loaded by placing samples in a separate dust-holding chamber. The dust sample is then injected into the test vessel through an air valve and across a rebound plate system Figure 2-13. Testing within the PRL 20L vessel utilized Sobbe chemical ignitors with a total energy of 2.5 kJ [16] [18].

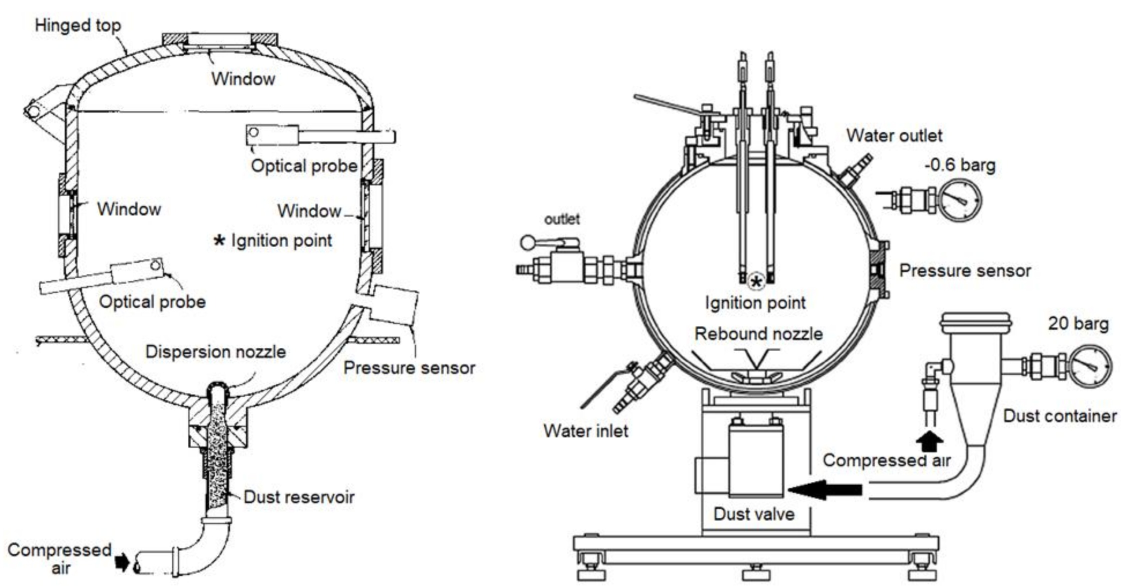


Figure 2-13. A Comparison of the USBM PRL 20L on Left (adapted from Cashdollar 1996) and the Siwek 20L on Right (adapted from KuhnerAG 2011)

Cashdollar in 2000 noted the PRL 20L chamber created low levels of turbulence during experimentation. It was stated that at the higher turbulence level recommended in ASTM Standard E1226-12A, the maximum $(dP/dt)V^{1/3}$and $K_{st}$ data would be roughly three times higher [12]. The increased turbulence helps create a homogenous dispersion of powder within the test vessel. It was also found that more turbulent flow decreases ignition delay and increases the rate of pressure increase through mixing of ignited dust particles, unignited dust particles, and heat generated by the combustion of the dust particles [6].

## 2.7. LITERATURE REVIEW SUMMARY

The literature review established the danger that coal dust explosions present to industry, what characteristics influence dust explosions, what testing has been done in the past, and how the historic testing differed from current testing standard procedures. The review identified a primary topic which needed to be studied. The topic of interest was PPC dust at high concentrations had not been assessed for explosive characteristics following ASTM E1226 testing standards.

# 3. PRELIMINARY INVESTIGATION INTO PPC COMBUSTIBILITY USING ASTM STANDARD E1226-12A

A greater part of this section has been published in Proceedings of the Combustion Institute [2] and Journal of Archives of Mining Sciences [2]. The preliminary investigation into PPC combustibility followed the test procedure outlined within the 20 L Apparatus Manual supplied with the Siwek 20L Sphere [28]. The tests conducted complied with ASTM E1226-12A. The Siwek 20L Sphere used for the testing can be seen in Figure 3-1. During an experiment, PPC dust was placed in the dust sample container and it was pressurized to 20 bar (gauge). The explosion chamber was connected to a vacuum pump and a pre-test pressure level of -0.6 bar (gauge) was set. The PPC dust was distributed from the dust container into the partially evacuated explosion chamber by remote activation of a solenoid valve at the base of the explosion vessel. The resulting dust cloud was ignited with two 5 kJ SOBBE chemical igniters placed at the end of the ignition leads. The igniters were located at the center of the spherical explosion chamber. Two Kistler piezoelectric pressure transducers were used to observe the pressure history from each test.

The Siwek 20L sphere was calibrated with niacin as part of the Calibration Round Robin of 2015 (CaRo15) sponsored by Adolf Kuhner AG. The niacin was milled, homogenized, and shipped in airtight packages. The niacin was evaluated per the procedure described in the Manual CaRo 15 [29]. Results from the preliminary explosive dust characterization test on the niacin can be seen in Table 3-1.

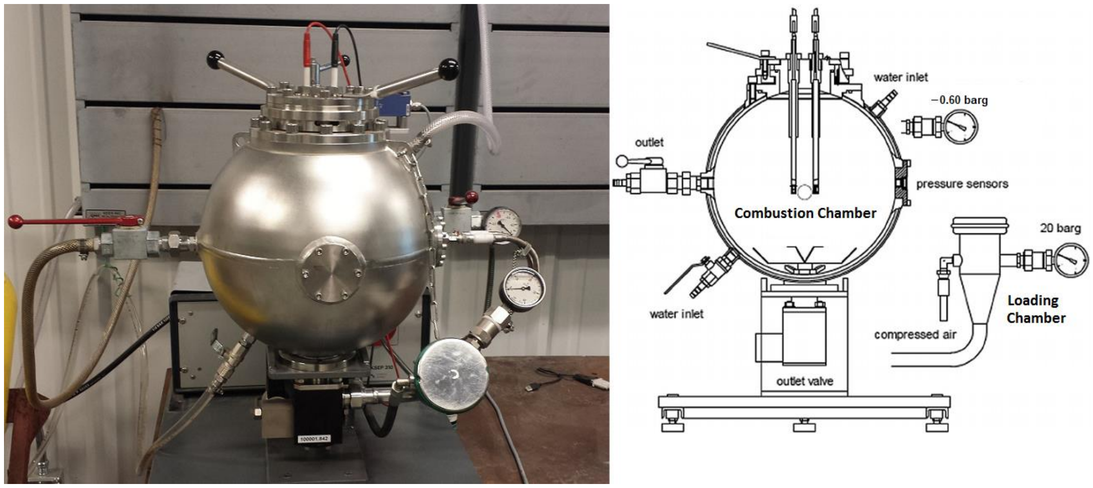


Figure 3-1. University Siwek 20L Sphere, modified from [3]

Table 3-1. Explosives Characteristics of Niacin from University Testing

| | |
|---|---|
| $P_{max}$ | = 8.4 bar |
| $(dP/dt)_{max}$ | = 923 bars/s |
| $(K_{st})_{max}$ | = 250 bar*m/s. |

Adolf Kuhner reported that 62 test laboratories worldwide submitted explosive dust characterization data on the niacin utilized during the Calibration Round Robin of 2015 [30]. There were 75 unique evaluations on the niacin, which resulted in reference values for $P_{max}$ and $K_{st}$ as shown in Table 3-2. The University's evaluation of the supplied niacin is within the published reference values. The Siwek 20L sphere is certified to function correctly by the Calibration Round Robin.

Table 3-2. CaRo 15 Reference Values [30]

| | | |
|---|---|---|
| $P_{max}$ (bar) | = 8.2 +/- 10% | 7.3 … 9.0 bar |
| $(K_{st})_{max}$ (bar*m/s ) | = 245 +/- 10% | 220 … 269 bar |

The distribution of the PPC used in the preliminary testing was evaluated by following ASTM Standard D197-87, Standard Test Method for Sampling and Fineness Test of Pulverized Coal [31]. ASTM standard D197 – 87 utilizes a standard set of sieves to create eight distinct size classifications. The results from this test can be seen in Table 3-3 . The University's PPC had a particle distribution with 39% minus 200 mesh and had a median diameter in between 150-µm and 75-µm size. The USBM tested coal with 80% minus 200 mesh and the median diameter was 48 microns.

Table 3-3. Results from ASTM D197-87 Analysis of PPC

| % Retained | Cumulative % Retained | Cumulative % Passing | sieve size | sieve (µm) |
|---|---|---|---|---|
| 0% | 0% | 100% | 8 | 2360 |
| 0% | 0% | 100% | 16 | 1180 |
| 0% | 0% | 100% | 30 | 600 |
| 4% | 4% | 96% | 50 | 300 |
| 27% | 30% | 70% | 100 | 150 |
| 31% | 61% | 39% | 200 | 75 |
| 15% | 76% | 24% | 325 | 45 |
| 24% | 100% | 0% | 325+ | 45- |

Dust samples were not sifted, sorted, or processed to change particle size or shape. To minimize particle size variation all test samples were pulled from the same container of PPC. The container of PPC was blended using a shaker-mixer technique in an effort to minimize particle segregation that may have occurred during shipping. Dust humidity levels were below 10% and kept consistent by storing all samples and material in sealed containers. The tests were conducted in an environmentally controlled laboratory with an ambient air temperature of 70 degrees Fahrenheit (21.1 degrees

Celsius). All testing was conducted with the same bottle of compressed air that had a tank pressure greater than 40 bar. The temperature and flow of the water through the 20 Liter Siwek Sphere water jacket was verified to be within specifications (< 25°C, and > 0.5 liter/minute). To control the effects of turbulence, the ignition delay time is standardized for the Siwek 20L Sphere at 60 milliseconds [28].

The test procedure outlined within the Siwek 20L manual [28] recommends an initial test series with dust masses and concentrations as seen in Table 3-4. The first test series starts at a low dust concentration of 60 g/m$^3$ and increases in steps to a high dust concentration of 1,500 g/m$^3$. This is so the maximum value for the explosion pressure ($P_{ex}$), and the rate of pressure increase, $(dP/dt)_{ex,}$ can clearly be determined.

Table 3-4. Dust Mass and Concentration Recommended for Testing in Siwek 20L Sphere [28]

| | | | | | | | | |
|---|---|---|---|---|---|---|---|---|
| Coal Dust Mass (g) | 1.2 | 2.5 | 5.0 | 10 | 15 | 20 | 25 | 30 |
| Coal Dust Concentration (g/m$^3$) | 60 | 125 | 250 | 500 | 750 | 1000 | 1250 | 1500 |

Test series two and three are conducted for replication. The replication of data is used to validate the complete dust evaluation. The $P_{ex}$ for each dust concentration level has a mean value calculated. If the $P_{max}$ from any of the three test series deviates more than 5% from the mean of the three test series, then the dust evaluation is invalid. If the $(dP/dt)_{ex}$ or $K_{st}$ from one test series deviates more than 20% from the mean of the three test series, then the dust evaluation is invalid. For this research the maximum mean value of peak pressure, rate of pressure change and explosive index is reported at $P_{max}$, $(dP/dt)_{max}$; and $(K_{st})_{max}$.

### 3.1. PRELIMINARY RESULTS FOR PPC DUST CONCENTRATIONS BETWEEN 60-1,500 g/m$^3$

Most of the PPC dust concentrations tested passed the criteria set in ASTM 1226-12A. The ASTM 1226-12A criteria states the $P_m$ and the $K_{st}$ should not deviate from the mean value for each concentration by 5% and 20% respectively. The dust concentration of 60 g/m$^3$ does not meet the criteria set for peak pressure, $P_m$, and may need retesting. The dust concentration of 60g/m$^3$ does not impact the maximum values for the dust explosion characteristics of $P_{max}$ or $(K_{st})_{max}$. Figure 3-2 presents an overview plot of the data collected during the preliminary testing.

From the data collected during the research and previously published [2], the $P_m$, corrected $P_{ex}$ from equation 2 [14] trends upward with increasing dust concentrations until a concentration of 250 g/m$^3$. The rise in the $P_m$ between dust concentrations of 200 and 500 g/m$^3$ is relatively constant. Beyond the dust concentration of 500 g/m$^3$ it can be seen that $P_m$ corrected trends downward. Identifying the maximum $P_m$ corrected between 250 and 500 g/m$^3$ has been identified as the first objective of the proposed research.

The $(dP/dt)_{ex}$ and its corresponding $K_{st}$ values will have more variability due to the nature of the testing conducted. The slightest change in turbulence, mixing, ignitor energy and ignition timing all affect the reaction rate of the dust explosion process. A best effort is made to keep the reaction variables constant but there is some inevitable variation. However, the $K_{st}$ data has more variability, and a trend is more difficult to discern than the pressure data.

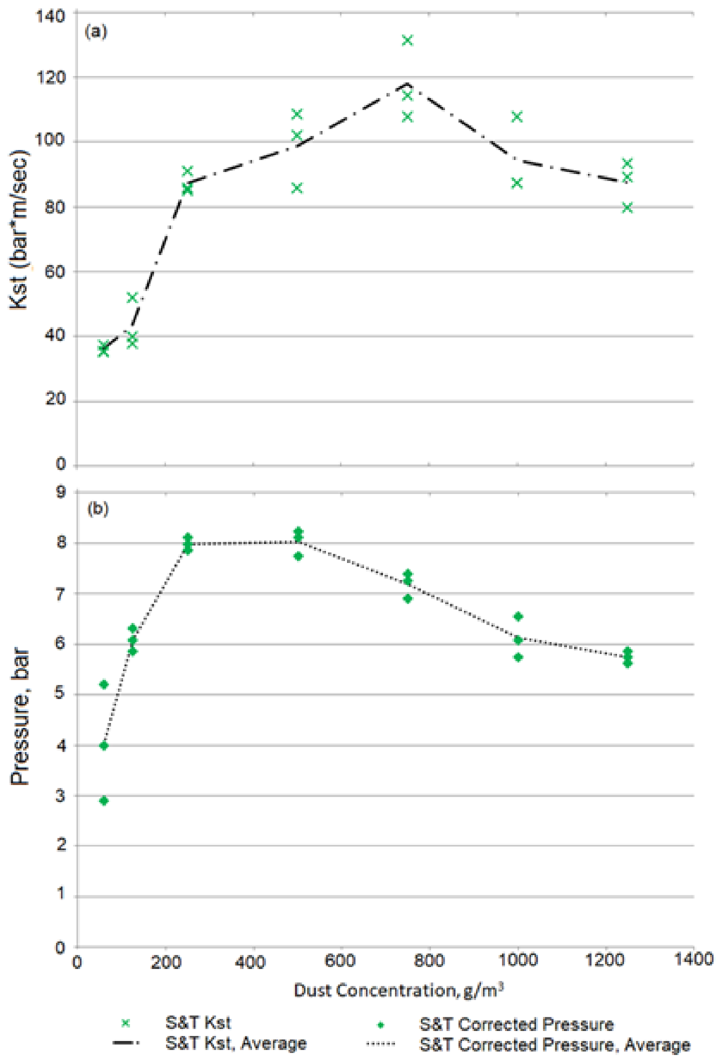


Figure 3-2. $P_{max}$ and $K_{st}$ for PPC Dust in University Siwek 20L Sphere [1]

The maximum explosive parameters from the evaluation of PPC can be seen in Table 3-5. . The maximum mean value of peak pressure, rate of pressure change and explosive index is reported at $P_{max}$, $(dP/dt)_{max}$; and $(Kst)_{max}$ per ASTM standards (ASTM E1226-12a, 2012). The $P_{max}$ value of 8.1 bar occurred at a concentration of 500 g/m$^3$. The $(K_{st})_{max}$ and $(dP/dt)_{max}$ are reached at a concentration of 750 g/m$^3$ with values of 118 bar*m/s and 435 bar/s respectively.

Table 3-5. Maximum Explosive Parameters of PPC

| | | |
|---|---|---|
| $P_{max}$ | = 8.1 bar | @ 500 g/m$^3$ |
| $(dP/dt)_{max}$ | = 435 bars/s | @ 750 g/m$^3$ |
| $(K_{st})_{max}$ | = 118 bar*m/s. | @ 750 g/m$^3$ |

When the Missouri S&T [2] results are compared against previously published data from the USBM [18] a few differences can be readily seen, Figure 3-3. Peak pressures recorded in the Siwek 20 L are consistently higher until the concentration level of 900 g/m$^3$ is reached. Higher concentrations resulted in lower peak pressure when compared to the referenced data. The Maximum corrected pressure reached in this research was 8.1 bars compared to approximately 6.6 bar reported by the USBM in [18]

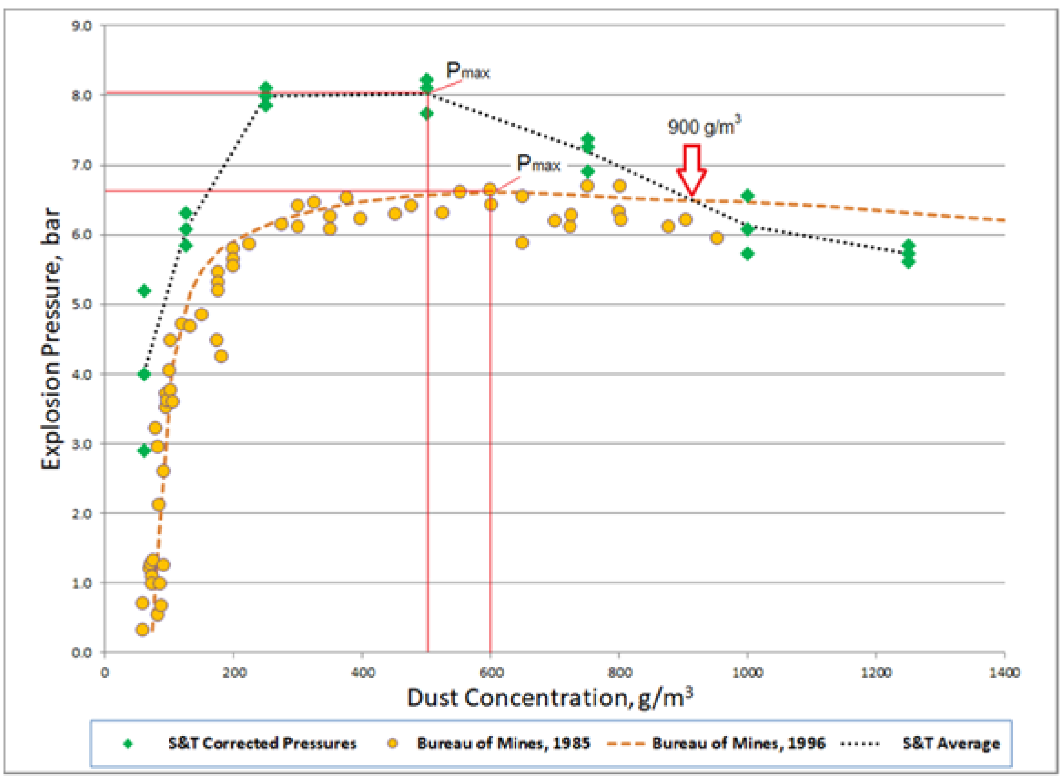


Figure 3-3. Explosion Pressure - S&T Data [2, 1] with Referenced Data [18] [16]

The trend lines vary a great deal as well. The research presented in the preliminary testing [2] shows a narrow range of pressure peak developing between concentrations of 250 and 500 g/m3. Additionally, the slope of decreasing pressure beyond $P_{max}$ descends at a steeper rate than the trend line published by the USBM in 1996 [16]. Both data sets are a tight fit to their respective trend lines. The USBM trend line from the [16] appears to be a good fit to the data presented [18]. In (Cashdollar, 1996) it is not explicitly stated that the trend line is related to any specific published data.

The differences in data trends seen in Figure 3-3 may be due to a couple factors. First, the 10 kJ chemical igniters that were used during the preliminary testing could account for the higher $P_{max}$, when compared to the USBM data that used 5 kJ ignitors. The preliminary testing's clearly defined pressure peak could be a result of the Siwek 20L vessel creating a more turbulent flow than the USBM PRL 20 liter vessel.

The $K_{st}$, explosive index, also varies greatly between the USBM published data and the preliminary testing, see Figure 3-4. The trends $K_{st}$ data is similar with the pressure data, in which the preliminary study had a magnitude of 3-4 times the values seen in the USBM data. A second order polynomial trend line shows a peak $K_{st}$ in the USBM data of around 30 bar*m/s, whereas the $(K_{st})_{max}$ in the preliminary study was approximately 120 bar*m/s. This is somewhat expected as Cashdollar states:

"Note that the turbulence level was lower in the PRL 20-L chamber for these tests than that recommended in ASTM E1226. At the higher turbulence level recommended in ASTM Standard E1226, the maximum $(dP/dt)V^{1/3}$ data for this Pittsburgh coal would be roughly three times higher." [12]

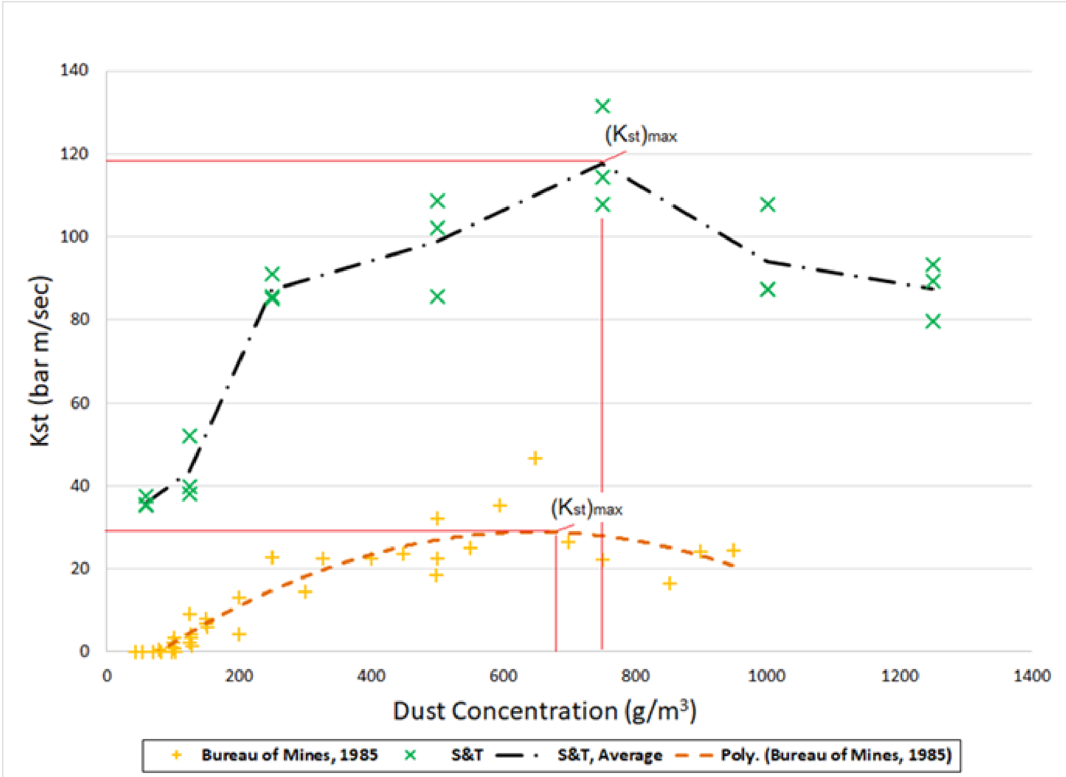


Figure 3-4. Explosion $K_{st}$ - University Data [2]with Referenced Data [18]

It was theorized that the preliminary test data would trend lower in all dust explosion characteristics compared to the USBM published data due to the larger PPC particle size present in the preliminary test. The data indicates this theory is incorrect. The preliminary test data trended higher than the USBM data. If the University had finer PPC, it is plausible that the $P_{max}$, $(dP/dt)_{max}$ and $K_{st}$ could all be higher than those recorded during testing.

## 3.2. PRELIMINARY RESULTS FOR PPC DUST CONCENTRATIONS BETWEEN 1,250-3,000 g/m$^3$

The prliminary testing for PPC dust concentrations between 60 and 1,500 g/m$^3$ indicated testing at higher concentrations with the Siwek 20L may also differ from the previously published USBM data for higher dust concentrations. Higher dust concentrations upto 3000 g/m$^3$ were tested by the University in a Siwek 20L vessel per ASTM E1226 at increasing concentrations of 250 g/m$^3$. The results of the PPC dust evaluation at higher dust concentrations can be seen in Figure 3-5.

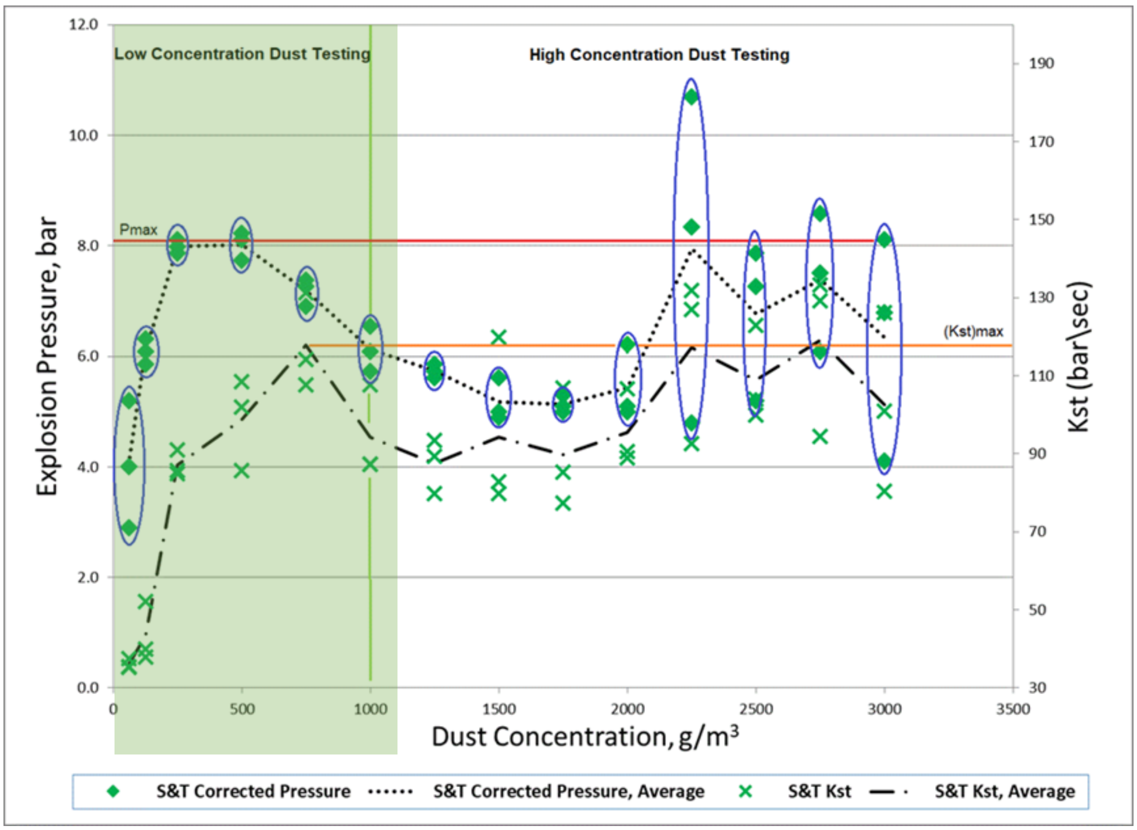


Figure 3-5. University PPC Explosive Dust Characteristic, Expanded Concentrations

The trend lines for the $P_{max}$ and $K_{st}$ initially track with what is to be expected based on trends previously published by Cashdollar, Mittal, and Woskoboenko [20] [16] [22]. Increasing dust concentrations produce lower pressure and $K_{st}$ values after the peak values for $P_{max}$ and $K_{st}$ was attained for concentrations of 500 g/m$^3$ and 750 g/m$^3$, respectively. This holds true to around a dust concentration of 2,000 g/m$^3$. For the dust concentrations examined beyond 2,000 g/m$^3$, pressure and $K_{st}$ have at least one data point equal to or greater than the maximum values recorded at lower concentrations. One particular explosion pressure at 1125 g/m$^3$ had a recorded magnitude of 11 bar. The literature reviewed for this research indicate a secondary peak would not be present as the dust concentrations increase.

The spread of the pressure data is contained by the blue ovals. For concentrations below 1,750 g/m$^3$ the data is fairly consistent with low variability. At dust concentrations of 2,000 g/m$^3$ and higher the deviation of recorded data becomes quite large. The $K_{st}$ and pressure data both have increased variability at higher concentrations compared to the low concentrations. This could be an indication that there are some parameters of the test procedure causing increased variability at high dust concentrations that is not apparent at lower concentrations.

## 3.3. SUMMARY OF PRELIMINARY TESTING

Peak pressures recorded in the Siwek 20 L were consistently higher until the concentration level of 900 g/m$^3$ was reached. The maximum corrected pressure reached in the preliminary low concentration testing was 8.1 bars compared to approximately 6.6 bar reported by the USBM in [18]. The USBM data had a $K_{st}$ of around 30 bar*m/s, whereas the $(K_{st})_{max}$ in the preliminary low concentration study was approximately 120 bar*m/s.

Increasing dust concentrations produce lower pressure and $K_{st}$ values after the peak values for $P_{max}$ and $K_{st}$ was attained for concentrations of 500 g/m$^3$ and 750 g/m$^3$, respectively. This held true to around a dust concentration of 2,000 g/m$^3$. Dust concentrations examined beyond 2,000 g/m$^3$ have at least one data point for pressure and $K_{st}$ equal to or greater than the maximum values recorded at lower concentrations. The $K_{st}$ and pressure data both have increased variability at higher concentrations compared to the low concentrations. This is indicative that some parameters of the test procedure caused increased variability at high dust concentrations that were not apparent at lower concentrations. The variability in test results at higher dust concentrations warranted further investigation and lead to experiments covered in the following section.

# 4. RESEARCH CONDUCTED

In the preliminary investigation for higher concentration, it was observed that the amount of coal present in the vessel and the loading chamber post evaluation increased as the dust concentrations increased. The presence of coal dust in the loading chamber could indicate that air classification occurred. If the introduction of the PPC is not uniform across dust concentrations it is plausible that the variations in $P_{max}$ and $K_{st}$ vary due to inconstant particle distribution in the vessel. Therefore, the objectives are designed to examine if the observed secondary peak in $P_{max}$ corresponds to the particle size distribution in a given sample at higher concentrations. The four objectives are seen below in Table 4-1.

Table 4-1. Overview of Objectives

| | **Objectives** |
|---|---|
| 1 | Identify Peak Pressure and dust concentration that creates peak pressure between 250 and 500 g/m$^3$. |
| 2 | Quantify dust particle size and distribution that is injected into the combustion chamber. |
| 3 | Quantify dust mass, particle size and distribution that is not injected into the combustion chamber and stays behind in loading chamber. |
| 4 | Identify if tight particle distribution correlates to explosion peak pressure and pressure trends vs dust concentration. |

This section outlines the test methods, results, and analysis for each of the stated objectives. Each objective, corresponding hypothesis, and investigation are grouped into distinctive sub-sections.

## 4.1. OBJECTIVE 1: IDENTIFY PEAK PRESSURE AND DUST CONCENTRATION THAT CREATES PEAK PRESSURE BETWEEN 250 AND 500 g/m$^3$

Testing was required to obtain a more accurate measurement of the coal dusts explosive parameters. The standard testing increments leave a range of concentrations unevaluated. The $P_m$ between dust concentrations of 200 g/m$^3$ and 500 g/m$^3$ is relatively constant and could indicate a higher pressure value may be between the tested concentrations. The hypothesis is that a higher $P_{max}$ exists between the initial dust concentrations evaluated following ASTM E1226. A more well-defined $P_{max}$ value is needed to compare higher dust concentrations reaction pressures with more precision. In Figure 4-1 the area of peak pressure is circled in red. A red arrow highlights a larger pressure value of 11 bar recorded at a higher dust concentration of 1125 g/m$^3$. The testing was required to discern weather a peak pressure, $P_{max}$, was missed at lower dust concentrations or if the pressure value of 11 bar denoted at higher dust concentrations is erroneous.

Concentrations between 250 and 500 g/m3 were evaluated in the Siwek 20L sphere. The dust mass required can be seen in Table 4-2. A minimum of 12 tests shots were required to complete this task.

Table 4-2. Coal Dust Mass and Concentration Required for Detailed Testing

| | | | | |
|---|---|---|---|---|
| Coal Dust Mass (g) | 6.0 | 7.0 | 8.0 | 9.0 |
| Coal Dust Concentration (g/m$^3$) | 300 | 350 | 400 | 450 |

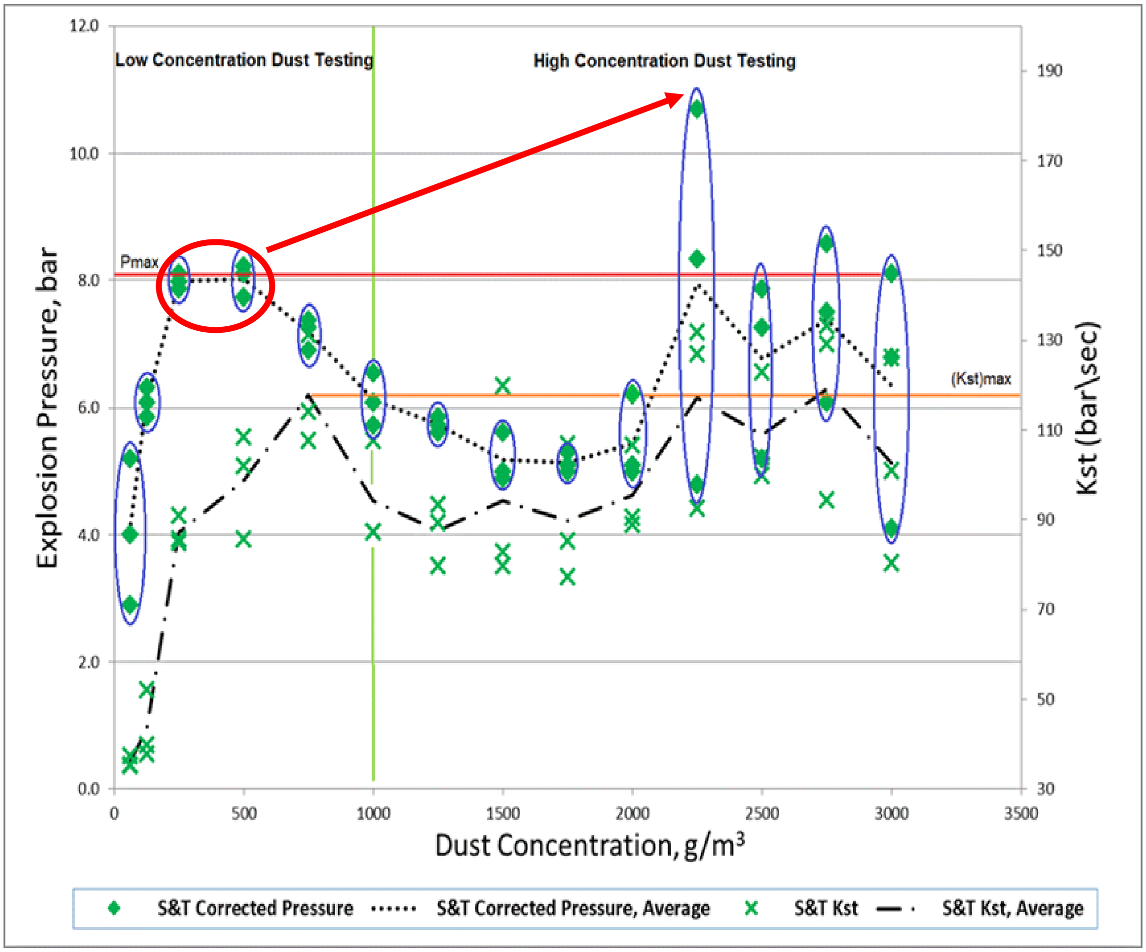


Figure 4-1. Conducted Coal Dust Testing. $P_{max}$ Area Circled in Red. Arrow Denoting Recorded Pressure of 11 bar at Higher Dust Concentration

The dust explosion pressure increases as dust concentration increases until a stoichiometric mixture was reached. Further increases in dust concentration result in the explosive pressure decreasing. In Figure 4-2 the converging trends are represented by red lines. Between the dust concentrations of 300 g/m$^3$ and 450 g/m$^3$ the red lines cross. The speculative $P_{max}$ should be around the plotted vertex near the dust concentration of 300 g/m$^3$.

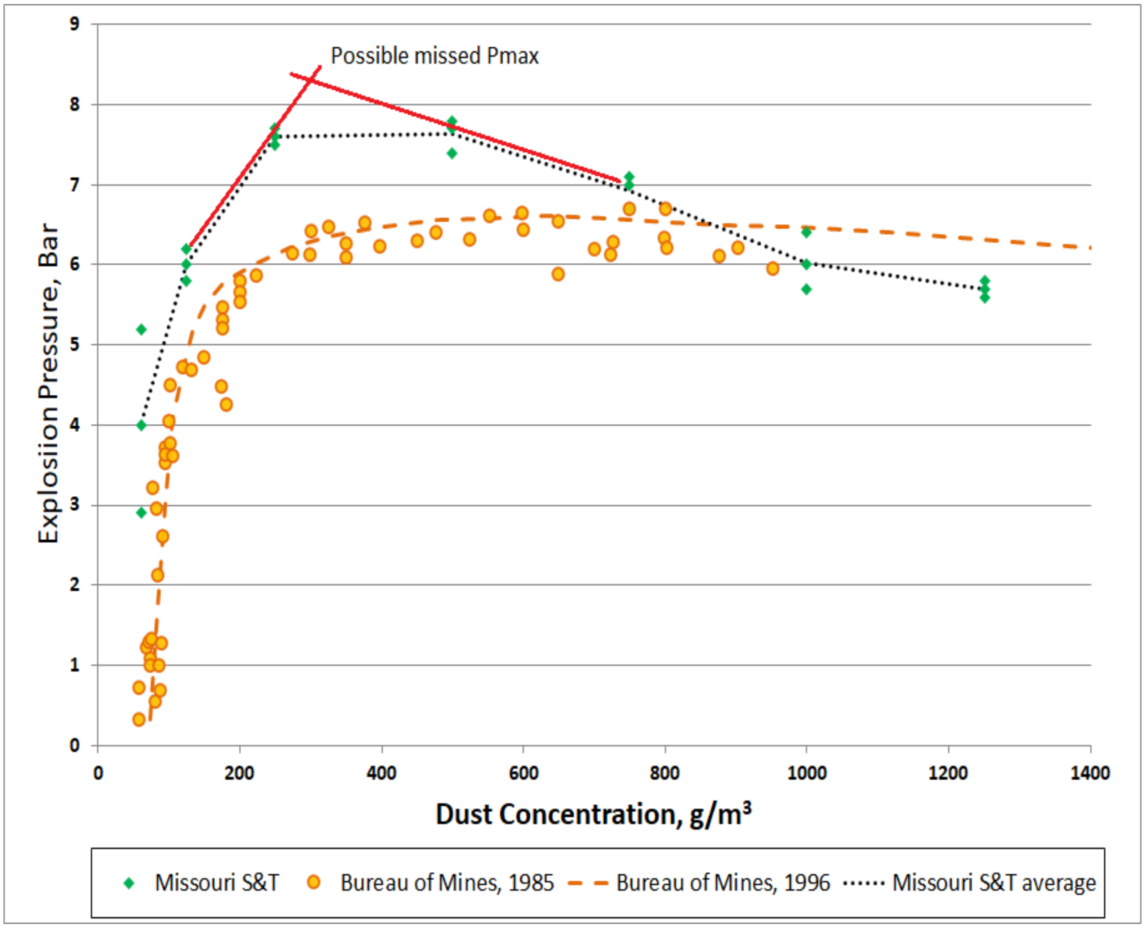


Figure 4-2. Converging Trends, Represented by Red Lines, Depict Possible $P_{max}$

**4.1.1. Data and Analysis**. Testing was conducted following the procedures described in Section 3. The new test data represented by red X's is illustrated in Figure 4-3. The initial PPC evaluation test series indicated that the maximum explosion pressure was 7.6 bar. The close concentration dust evaluation revealed a maximum explosion pressure, $P_{max}$, of 7.8 bar at a dust concentration of 350 g/m$^3$. During testing, it was noticed that an unknown quantity of dust sometimes remained in the loading chamber.

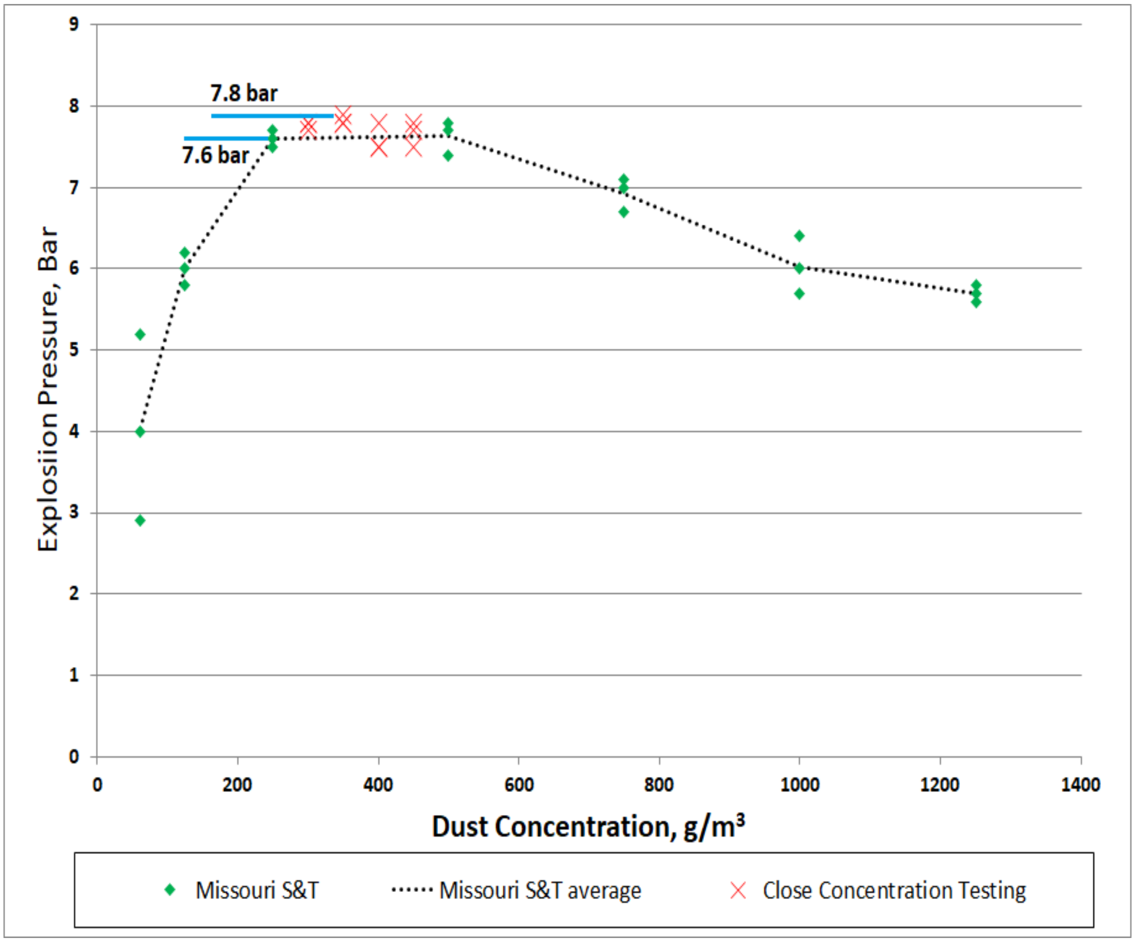


Figure 4-3. Initial PPC Evaluation Test Data with New Data Shown in Red "X"s

**4.1.2. Objective 1 Findings.** A more accurate value for $P_{max}$ was recorded between the dust concentrations of 250 and 500 g/m$^3$. At a dust concentration of 350 g/m$^3$ a peak pressure of 7.8 bar was recorded. The new $P_{max}$ value of 7.8 bar is not significantly greater than the value of 7.6 bar recorded following the manufacturer's recommended testing procedures of the Siwek 20L vessel. The $P_{max}$ value of 7.8 bar is lower than the pressure of 11 bar recorded once at a higher dust concentration of 1,125 g/m$^3$. A review of objective 1, hypotheses, and findings can be seen in Table 4-3.

Table 4-3. Summary of Objective 1

| | |
|---|---|
| **Objective** | |
| 1 | Identify Peak Pressure and dust concentration that creates peak pressure between 250 and 500 $g/m^3$. |
| **Hypotheses** | |
| | Peak pressure will be between 250 and 500 $g/m^3$. Actual peak pressure will be higher than pressures recorded at 250 and 500 $g/m^3$. |
| **Findings** | |
| | Peak pressure was between 250 and 500 $g/m^3$. $P_{max}$ of 7.8 bar is not significantly greater than the value discovered during initial testing. PPC material was left in loading chamber. The pressure reading of 11 bar at 1125 $g/m^3$ is due to an unknown error. |

## 4.2. OBJECTIVE 2: QUANTIFY DUST MASS, PARTICLE SIZE AND DISTRIBUTION THAT IS INJECTED INTO THE COMBUSTION CHAMBER

A greater part of this section has been published in , Powder Technology [3]. This testing will show if secondary comminution is occurring during dust injection and distribution thus shifting the dust size distribution. The test will also indicate if there are quantities of dust not being injected into the combustion chamber thus changing the effective dust concentration evaluated. The actual dust mass and size distribution needs to be known. The pressure vs concentration curve may need to be shifted. The particle size and distribution effect the combustion rate. If the shift in particle size and distribution is not consistent across dust concentrations tested, the dust explosion characteristics could be affected.

To evaluate objective two the concentrations of dust initially tested from 125 to 3,000 $g/m^3$ in the Siwek 20L vessel per ASTM E1226 were rerun without the ignitors. The dust mass and concentrations can be seen in Table 4-4. Each concentration was evaluated 3 times. After each test shot the dust from the combustion chamber and the loading chamber was recovered separately. Each posttest dust sample had its mass, and particle size distribution analyzed. A minimum of 39 test shots were required to complete this task.

Table 4-4. Coal Dust Mass and Concentration Required for Expanded ASTM E1226 Evaluation

| | | | | | | | | | | | | | |
|---|---|---|---|---|---|---|---|---|---|---|---|---|---|
| Coal Dust Mass (g) | 2.5 | 5.0 | 10 | 15 | 20 | 25 | 30 | 35 | 40 | 45 | 50 | 55 | 60 |
| Coal Dust Concentration ($g/m^3$) | 125 | 250 | 500 | 750 | 1000 | 1250 | 1500 | 1750 | 2000 | 2250 | 2500 | 2750 | 3000 |

In Figure 4-4 a general flow diagram can be seen. Each dust sample went through the same steps. A mass of powder listed in Table 4-4 was loaded into the dust container on the Siwek 20L. The dust was dispersed into the Siwek 20L apparatus using the manufacturer supplied control software. After each dust dispersion, the test apparatus was taken apart at the isolation valve. A sample cup was placed under the now exposed inlet port on the bottom of 20-L vessel. The rebound nozzle was cleaned and removed from the interior of the 20-L vessel. A camel hair brush was used to gently clean and sweep all injected dispersion material into the inlet port and down into the sample cup below. Each concentration, mass quantity, was evaluated three times, each time with new PPC. No PPC material was injected more than once.

All post dispersion samples were processed individually through a micro rotary riffler before particle size analysis, as seen in Figure 4-4. The rotary riffler's vibrator bowl automatically fed material to provide eight representative powder samples in rotating sample tubes in front of the vibrator. The process met ASTM Standard D197-19 requirements to ensure that the sub-samples accurately represent the characteristics of the large powder quantity that they correspond to [31].

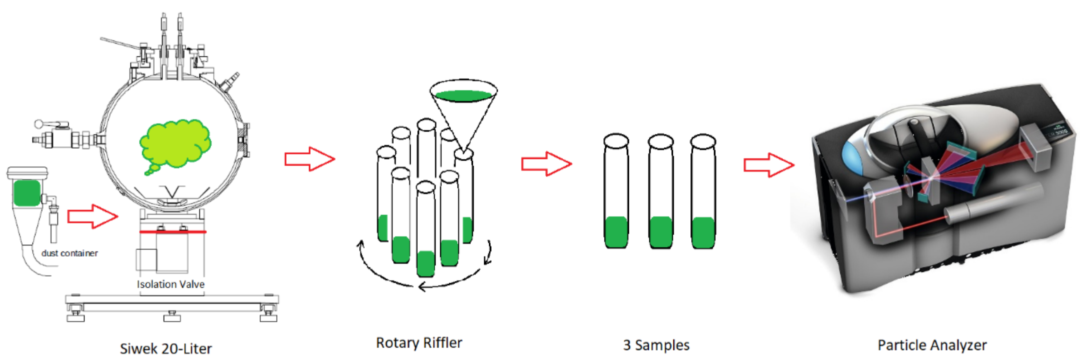


Figure 4-4. Dust Sample Processing Flow from Loading to Particle Analysis

For each unique post dispersion material sample, three of the riffler's eight representative powder samples were analyzed for particle size, size quantity, and distribution. A Malvern Mastersizer 3000 laser diffraction particle size analyzer was used to measure the particle size distribution and calculate distribution statistics of each post dispersion sample. The PPC feedstock was measured by the author applying the same sampling and measurement processes used on post dispersion samples.

**4.2.1. Injected Dust Results and Discussion.** PPC was used within a Siwek 20L test apparatus and post dispersion materials were collected and analyzed for particle size distribution. The measured particle distribution statistics of D10, D50 (median), D90, D(3,2), Span, skewness ($Sk_G$), as well as the changes in particle size distribution for the original feedstock and post test samples, can be seen in Table 4-5.

The statistic denoted by D10 is the diameter at which 10 percent of the sample's mass is comprised of particles with a diameter less than the reported value. A D50 value is the diameter size below which 50 percent of the material is contained. In similar fashion, 90 percent of the distribution lies below the D90 value. D(3,2) indicates the particle size with the mean surface area of the analyzed sample. The Span is defined as (D90 – D10)/D50 and gives an indication of how far the 10 percent and 90 percent points are apart, normalized with the midpoint [32]. Skewness ($Sk_G$) a mathematical expression that describes the preferential spread of particle size distribution away from the average. A negative $Sk_G$ value means the distribution is shifted to the left with more fine particles while a positive value indicates a larger quantity of large particles. $Sk_G$ is calculated using the Modified Folk & Ward graphic method presented in papers authored by Tascón, Blott, and Pye [33] [34].

$$Sk_G = \frac{lnD_{16}+lnD_{84}-2\ lnD_{50}}{2(lnD_{84}-lnD_{16})} + \frac{lnD_5+lnD_{95}-2\ lnD_{50}}{2(lnD_{95}-lnD_5)} \quad (3)$$

The loaded mass and equivalent dust concentrations can be seen on the left side of Table 4-5. The mass labeled Feed Stock is PPC dust before injection into and dispersion within the 20-liter vessel. All particle distribution statistics decrease for post-dispersion samples except for Span and Skewness. Span and Skewness increased for all post-dispersion samples. The lowest dust concentrations had the greatest change in particle size and distribution. The largest dust concentrations had the least change in measured powder characteristics.

Table 4-5. Mean Dust Characteristics for Pre and Post-dispersion PPC in a Siwek 20L Test Apparatus

| Mass Loaded (g) | Dust Concentration ($g/m^3$) | D10 (µm) | D10 Min (µm) | D10 Max (µm) | Median / D50 (µm) | D50 Min (µm) | D50 Max (µm) | D90 (µm) | D90 Min (µm) | D90 Max (µm) | % Decrease D10 | % Decrease D50 | % Decrease D90 | D(3,2) (µm) | % Decrease D(3,2) | Span, $\sigma_D$ | % Increase Span | Skewness, $Sk_G$ |
|---|---|---|---|---|---|---|---|---|---|---|---|---|---|---|---|---|---|---|
| Feed Stock | - | 15.70 | - | - | 98.4 | - | - | 268 | - | - | - | - | - | 124.0 | - | 2.56 | - | -0.292 |
| 2.5 | 125 | 3.81 | 3.70 | 4.02 | 24.9 | 23.8 | 26.4 | 107 | 97 | 115 | 75.7 | 74.7 | 60.1 | 44.2 | 64.4 | 4.14 | 61.7 | -0.125 |
| 5 | 250 | 4.19 | 4.14 | 4.28 | 28.3 | 27.8 | 28.6 | 114 | 109 | 121 | 73.3 | 71.2 | 57.5 | 46.6 | 62.4 | 3.88 | 51.6 | -0.158 |
| 10 | 500 | 4.89 | 4.87 | 4.92 | 35.5 | 35.3 | 35.9 | 149 | 148 | 151 | 68.9 | 63.9 | 44.4 | 59.2 | 52.3 | 4.06 | 58.6 | -0.165 |
| 15 | 750 | 5.41 | 5.28 | 5.55 | 41.5 | 40.6 | 42.5 | 171 | 170 | 171 | 65.5 | 57.8 | 36.2 | 67.4 | 45.6 | 3.99 | 55.9 | -0.186 |
| 20 | 1000 | 5.90 | 5.85 | 5.97 | 46.5 | 45.7 | 47.1 | 183 | 179 | 187 | 62.4 | 52.7 | 31.7 | 73.6 | 40.6 | 3.81 | 48.8 | -0.207 |
| 25 | 1250 | 6.32 | 6.20 | 6.55 | 49.9 | 49.0 | 50.5 | 192 | 189 | 196 | 59.7 | 49.3 | 28.4 | 77.0 | 37.9 | 3.72 | 45.3 | -0.215 |
| 30 | 1500 | 6.64 | 6.53 | 6.73 | 53.4 | 52.4 | 54.4 | 199 | 189 | 205 | 57.7 | 45.7 | 25.7 | 81.4 | 34.4 | 3.6 | 40.6 | -0.230 |
| 35 | 1750 | 6.56 | 6.01 | 6.91 | 54.6 | 52.8 | 56.3 | 209 | 207 | 211 | 58.2 | 44.5 | 22.0 | 84.4 | 31.9 | 3.71 | 44.9 | -0.228 |
| 40 | 2000 | 7.19 | 6.90 | 7.52 | 59.2 | 57.9 | 59.9 | 214 | 209 | 218 | 54.2 | 39.8 | 20.1 | 87.9 | 29.1 | 3.49 | 36.3 | -0.244 |
| 45 | 2250 | 7.47 | 7.19 | 7.62 | 60.5 | 59.0 | 61.6 | 216 | 214 | 221 | 52.4 | 38.5 | 19.4 | 89.0 | 28.2 | 3.45 | 34.8 | -0.247 |
| 50 | 2500 | 7.58 | 7.38 | 7.78 | 62.2 | 61.2 | 63.6 | 223 | 214 | 233 | 51.7 | 36.8 | 16.8 | 92.3 | 25.6 | 3.46 | 35.2 | -0.248 |
| 55 | 2750 | 8.00 | 7.77 | 8.20 | 66.1 | 63.6 | 68.3 | 234 | 226 | 241 | 49.0 | 32.8 | 12.7 | 97.7 | 21.2 | 3.42 | 33.6 | -0.252 |
| 60 | 3000 | 7.92 | 7.71 | 8.13 | 64.9 | 62.9 | 66.6 | 229 | 223 | 233 | 49.6 | 34.0 | 14.6 | 95.3 | 23.1 | 3.41 | 33.2 | -0.253 |

Figure 4-5 shows the particle distribution statistics of D10, D50 (median), and D90, with feedstock values presented by the dashed horizontal lines. The largest distance between the feedstock lines and dispersed PPC concentrations can be seen on the left of the plot with the smallest concentrations. At 125 $g/m^3$ the post dispersion D90 is almost equal to the feedstocks D50. The D50 of the 125 $g/m^3$ is close to the feedstock D10. At the lowest concentration of 125 $g/m^3$ D10, D50, and D90 were decreased by 76%, 75%, and 60% respectively compared to the feed stock. The PPC concentration of 2750 $g/m^3$ had a decrease of 49%, 33%, and 13% for D10, D50, and D90. Overall, as tested dust concentrations increased, the change in the post dispersion PPC particle size decreased. A potential reason for this is the Siwek 20L test apparatus is operated with the same positive and negative pressure in the loading and testing chamber respectively, regardless of the mass of material being tested. Since the energy available to accelerate the dust is constant, more energy would be applied to an individual particle at lower concentrations.

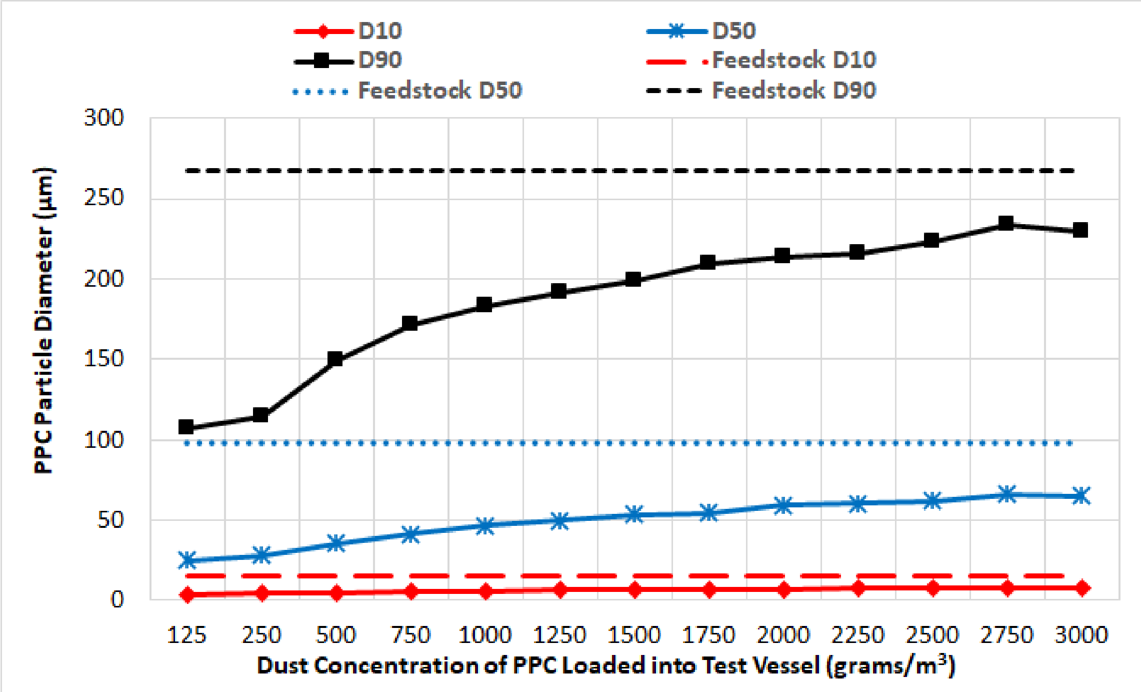


Figure 4-5. Dust Particle Size Statistics for all PPC Dust Concentrations Tested Along with Feedstock (Dashed Lines are Feedstock Values)

The dust concentration of 3,000 g/m$^3$ does not follow the particle size trends seen with the rest of the PPC dust analysis. Figure 4-5 shows a general trend where the smallest concentrations dispersed had the most comminution and the greatest change in D10, D50, D90. Each subsequent increase in dust concentration resulted in less change in the dust particle size and distribution. The trend follows up to 2,750 g/m$^3$. At 3,000 g/m$^3$ all dust statistics decreased which could indicate the trend may start reversing and more comminution is occurring. Dust concentrations beyond 3,000 g/m$^3$ are not practical as the loading chamber of the Siwek 20L apparatus cannot physically hold much more PPC dust and function as designed. The U.S. Bureau of Mines report had a maximum dust concentration of approximately 3,000 g/m$^3$ [16]. This work concludes that a concentration of 3,000 g/m$^3$ is 5 times the concentration corresponding to maximum reaction pressure [16, 30].

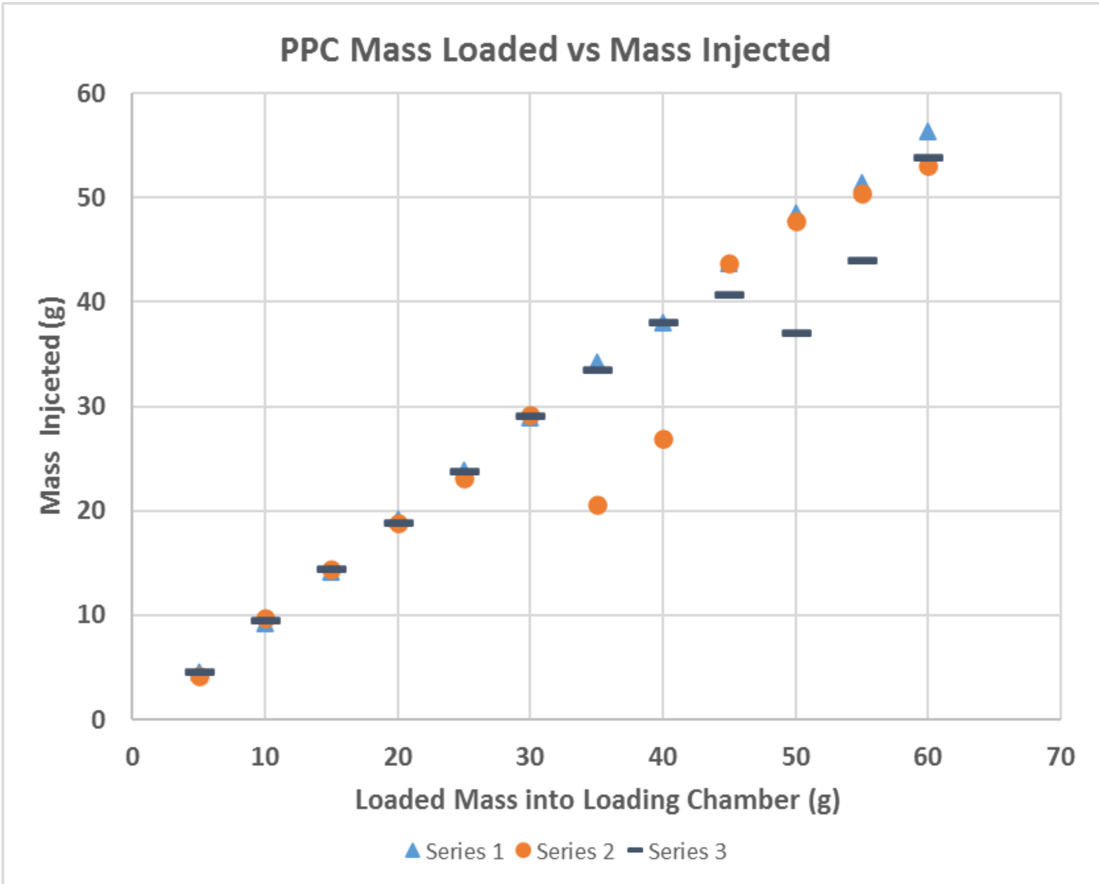


Figure 4-6. Mass of PPC Dust Injected into Combustion Chamber

The mass of PPC dust injected into the combustion chamber of the 20-L vessel was recorded for each test shot and the data can be seen in Figure 4-6. At lower masses, dust concentrations the mass injected is close to the mass loaded into the loading chamber. At loads above 30 grams of PPC dust the quantity of material injected does not repeat consistently between test series. There are four instances where 10 or more grams of loaded PPC dust was not collected from the combustion chamber after injection.

In Figure 4-7 the data is plotted based on the percentage of recovered PPC mass to loaded mass. The lower concentrations tested with masses below 25 grams had 90 percent or more with an average of approximately 95 percent of the powder injected and recovered. In one individual test at 5 grams approximately 84 percent of the loaded mass was recovered. At test quantities of 30 grams and greater the quantity of mass injected and recovered had higher variability. In four instances 80 percent or less of the loaded material was recovered from the combustion chamber. The four instances discussed are directly correlated to the four test shots missing 10 grams or more plotted in Figure 4-6.

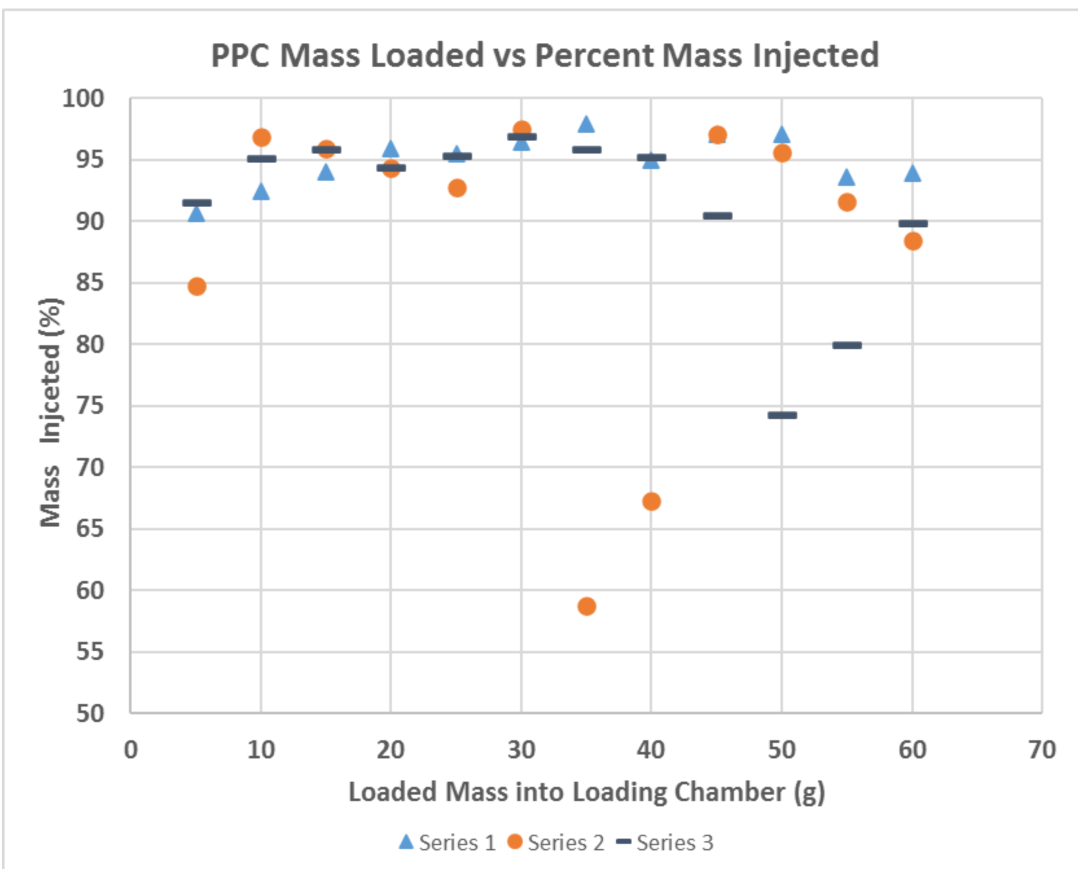


Figure 4-7. Percentage of Mass Injected into Combustion Chamber

The PPC dust mass missing from the combustion chamber will result in explosive characteristic testing data conducted on lower mass and concentrations than expected based on loaded mass quantities. In some instances a loaded mass of 40 or 50 grams will actually be evaluating the explosive characteristics of a PPC mass of 25 or 35 grams respectively

Figure 4-8 plots cumulative particle size distribution along with the original PPC feedstock particle diameters. For illustrative purposes only four dust concentrations are plotted to decrease crowding. The general trend is consistent for all dust concentrations. Within this plot, the cumulative volume percentage can be found for each of the represented dust concentrations.

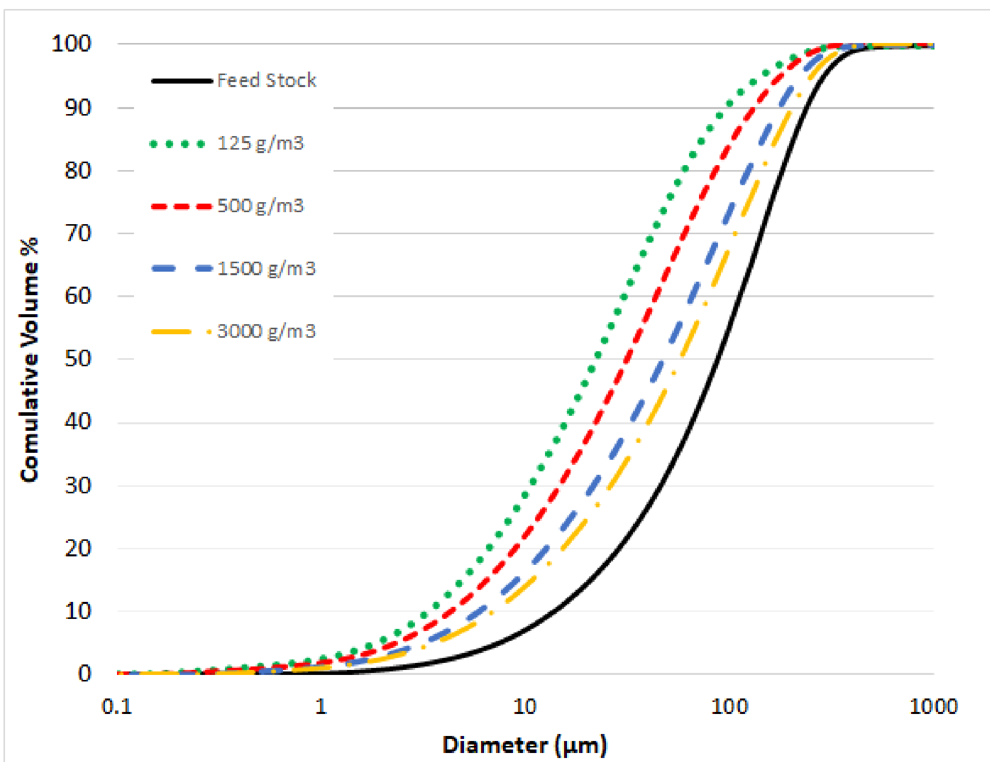


Figure 4-8. Cumulative Particle Size Distribution of Pre and Post-dispersion of PPC at Different Concentrations

Figure 4-8 shows the lowest concentration to the farthest left of the feedstock distribution. The low-density dust concentration had the most change in particle size. Each subsequent increase in dust concentration shifts slightly to the right and closer to the feedstock profile. All dust concentrations dispersed within the Siwek 20L vessel had an over-all decrease in particle size due to comminution during injection and dispersion.

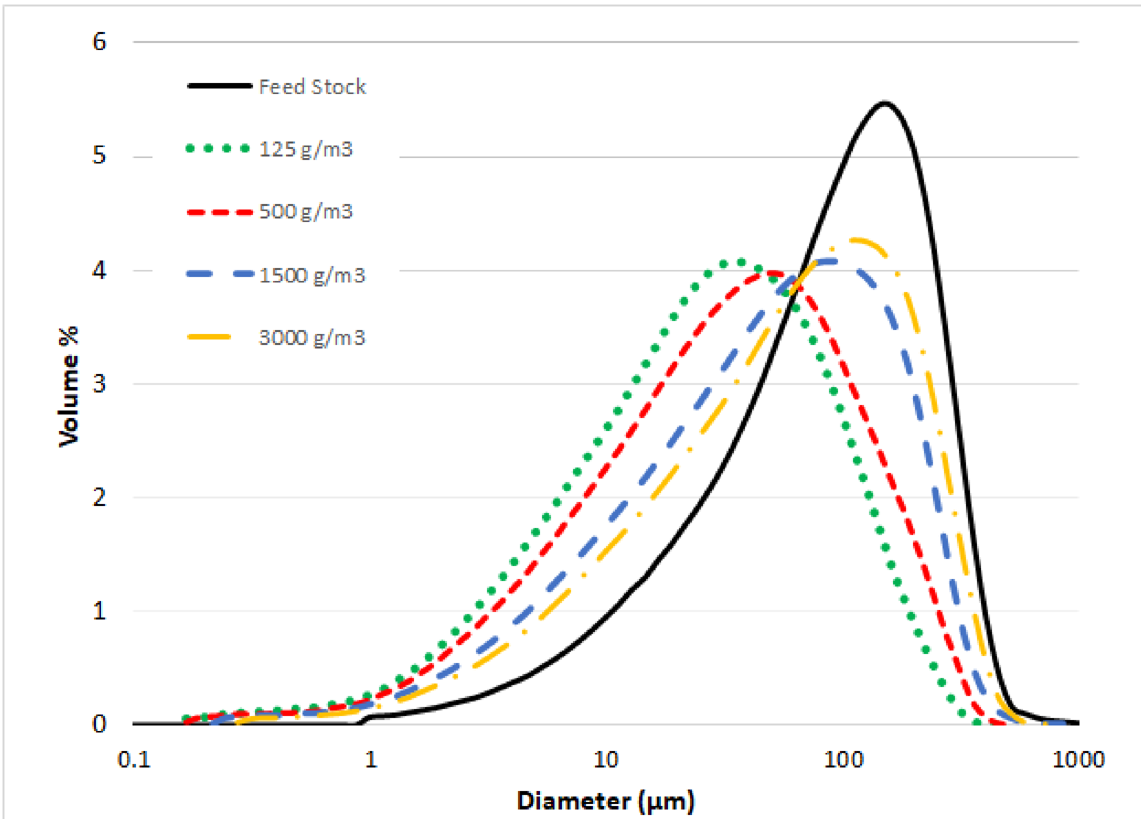


Figure 4-9.The Particle Size Distribution of Pre and Post-dispersion at Different Concentrations

Figure 4-9. plots particle size distribution by volume percentage of total sample volume for the same four representative dust concentrations and feed stock. Low-density dust concentrations are shifted to the left more than high-density dust concentrations.

This shift indicates the feedstock is reduced in size significantly by comminution during the injection and dispersion of the dust within the 20-liter apparatus. The specifics of the change can be calculated by the percent decrease of the D(3,2). Lower concentrations have a change of D(3,2) above 60 percent, while the highest concentrations evaluated had a change of approximately 20 percent. The percentage of change in D(3,2) decreases with the increase of dust concentration being tested.

The peak of each curve in Figure 4-9 corresponds with the median D50 of each data series. The lowest dust concentration of 125 g/m$^3$ departed the most from the feedstocks median D50 value. As dust concentrations increased the D50 approaches the values measured in the feedstock.

It can be seen on the lower left side of Figure 4-9 that more fine dust particles were present compared to the feedstock plot in black. The feedstock had no dust particles below 1 micron. All dispersed PPC had measurable quantities of material smaller than 1 micron. The left most extreme end of Figure 4-9 shows the smallest measured dust particle size increases conversely with dust concentrations. Similarly, the extreme right side of Figure 4-9 shows all dispersed PPC had maximum particle sizes shift to smaller diameters. Graphically, all particle size distributions for dispersed PPC shift left and lower than the feedstock.

The combination of the particle distribution shifting resulted in the Skewness of the dispersed PPC moving in a positive direction, closer to a value of zero. Typically, one would assume that an increase in fines could lead to a more energetic reaction and higher (dP/dt) values, as described by Eckhoff [6]. Tascón reported that as Skewness shifted in a positive direction, (dP/dt) values decrease [33]. The data presented within this dissertation does not refine the relationship between the two different trends in particle distribution characteristics vs. reaction rates.

**4.2.2. Objective 2 Findings.** Dust explosions are a major safety concern for industry. The explosion and fires following dust explosions can result in significant property damage and loss of life. The testing of PPC, a standard certification material for ASTM E1226, within a Siwek 20L apparatus resulted in the dust undergoing comminution meaning the actual dust characteristics evaluated are different than the feedstock loaded into the test vessel. This results in an unknown and unquantified bias or error. The bias could result in more energetic reactions and lead to the introduction of a safety factor into subsequent safety designs. Conversely, if the bias results in a less energetic reaction, then an undue risk may be present. Either way the bias makes computer modeling of energetic dust reactions difficult because the secondary comminution is not accounted for in thermodynamic and chemical reaction simulations. Further studies are recommended to fully understand the correlation between the comminution versus dust explosion characteristics and determine a safety factor.

The comminution occurs during the injection and dispersion of the samples into the Siwek 20L apparatus. All dust concentrations tested had D10, D50, D90, and D(3,2) values lower than the feedstock used. Lower dust concentrations underwent a greater change than higher dust concentrations, likely due to the equivalent energy used to disperse the dust. Lower dust concentrations had D10, D50, D90, and D(3,2) values 75% to 50% smaller than the feedstock. All dispersed dust samples had more fines and smaller particles than the feedstock. There is an indication that at very high dust concentrations, 3,000 g/m$^3$, the overall trend of comminution and particle size reduction may no longer be consistent with these trends. The work conveyed within this section was published in Powder Technology [3]. Table 4-6 reviews the hypotheses and findings related to objective 2.

Table 4-6. Summary of Objective 2

| | |
|---|---|
| **Objective** | |
| 2 | Quantify dust particle size and distribution that is injected into the combustion chamber. |
| **Hypotheses** | |
| | The particle size and distribution of dust injected is different than the feedstock's distribution. Injected dust will have more fine particles than feedstock. Low concentrations will have more fines by percent total mass than large concentrations due to the energy input into the system is constant for all concentrations. |
| **Findings** | |
| | Particle size and distribution of injected dust contains more fines than feedstock material. Low dust concentrations have more fines by percent total mass than large concentrations. |

## 4.3. OBJECTIVE 3: QUANTIFY DUST MASS, PARTICLE SIZE AND DISTRIBUTION THAT IS NOT INJECTED INTO THE COMBUSTION CHAMBER AND REMAINS IN LOADING CHAMBER

This testing was designed to show if air classification is occurring during dust injection and distribution thus shifting the dust size distribution. It is hypothesized that larger particles are not injected consistently because they are more prone to fall out of suspension when air flows from the loading chamber to the explosive testing chamber. The actual dust mass and size distribution needs to be known. If larger particles are not consistently injected into the 20 L vessel, then the shift in particle size noted in Section 4.2 is not solely due to secondary communication.

The concentrations of dust initially tested from 125 to 3,000 g/m$^3$ in the Siwek 20L vessel per ASTM E1226 were rerun without the ignitors. The dust mass and concentrations can be seen in Table 4-7. Each concentration was evaluated 3 times. After each test shot the dust from the combustion chamber and the loading chamber was recovered separately. Each posttest dust sample had its mass, and particle size distribution analyzed. A minimum of 39 test shots are required to complete this task. The dust analyzed within this test series is directly correlated to the dust from Section 4.2. For each mass injected into the combustion chamber there was a mass of dust recovered from the loading chamber. The dust sample processing and analysis utilized within this Section is the same used within Section 0.

Table 4-7. Coal Dust Mass and Concentration for Expanded ASTM E1226 Evaluation

| Coal Dust Mass (g) | 5 | 10 | 15 | 20 | 25 | 30 | 35 | 40 | 45 | 50 | 55 | 60 |
|---|---|---|---|---|---|---|---|---|---|---|---|---|
| Coal Dust Concentration (g/m$^3$) | 250 | 500 | 750 | 1000 | 1250 | 1500 | 1750 | 2000 | 2250 | 2500 | 2750 | 3000 |

**4.3.1. Dust Not Injected Results and Discussion.** PPC was used within a Siwek 20L test apparatus and materials left within the loading chamber were collected and analyzed for particle size distribution. The recovered mass of PPC not injected into the combustion chamber is plotted in Figure 4-13. The percentage of material not injected can be seen in Figure 4-14. The measured particle distribution statistics of D10, D50 (median), D90, D(3,2), Span, skewness ($Sk_G$), as well as the changes in particle size distribution for the original feedstock and post test samples can be seen in Table 4-5.

The loaded mass and equivalent dust concentrations can be seen on the left side of Table 4-8. The mass labeled Feed Stock is PPC dust before injection. Particle distribution statistics including Span and Skewness increased for most sample materials not injected. The D90 value decreased for some dust concentrations and increased for others. The percent change in the D90 values was not as significant the changes seen in D10 and D50. The change in particle size and distribution was fairly consistent across all dust concentrations. The smallest dust concentration of 750 g/m$^3$ had lower values for D10, D50, and D90 than other dust concentrations.

Table 4-8. Mean Dust Characteristics for Pre-dispersion PPC and Material Remaining in the Siwek 20L Loading Chamber

| Mass Loaded (g) | Dust Concentration (g/m$^3$) | D10 (µm) | D10 Min (µm) | D10 Max (µm) | Median / D50 (µm) | D50 Min (µm) | D50 Max (µm) | D90 (µm) | D90 Min (µm) | D90 Max (µm) | % Change D10 | % Change D50 | % Change D90 | D(3,2) (µm) | % Decrease D(3,2) | Span, $\sigma_D$ | % Decrease Span | Skewness, $Sk_G$ |
|---|---|---|---|---|---|---|---|---|---|---|---|---|---|---|---|---|---|---|
| Feed Stock | - | 15.70 | | | 98.4 | | | 268 | | | - | - | - | 124.0 | - | 2.56 | | -0.292 |
| 15 | 750 | 16.30 | 14.9 | 17.8 | 89.9 | 84.6 | 96.7 | 227 | 208 | 243 | -3.8 | 8.6 | 15.3 | 33.9 | 72.7 | 2.35 | 8.40 | -0.296 |
| 20 | 1000 | 27.60 | 25.8 | 28.9 | 107.0 | 96.3 | 114.0 | 255 | 203 | 377 | -75.8 | -8.7 | 4.9 | 49.6 | 60.0 | 2.13 | 16.68 | -0.215 |
| 25 | 1250 | 28.70 | 23.9 | 40.1 | 112.0 | 96.5 | 122.0 | 255 | 234 | 271 | -82.8 | -13.8 | 4.9 | 52.5 | 57.7 | 2.03 | 20.82 | -0.250 |
| 30 | 1500 | 23.80 | 21.5 | 27 | 111.0 | 110.0 | 111.0 | 257 | 248 | 264 | -51.6 | -12.8 | 4.1 | 44.9 | 63.8 | 2.11 | 17.66 | -0.295 |
| 35 | 1750 | 22.70 | 20.7 | 25.8 | 107.0 | 104.0 | 111.0 | 266 | 257 | 281 | -44.6 | -8.7 | 0.7 | 44.4 | 64.2 | 2.28 | 11.02 | -0.258 |
| 40 | 2000 | 22.90 | 19.6 | 26.4 | 109.0 | 104.0 | 112.0 | 273 | 261 | 299 | -45.9 | -10.8 | -1.9 | 44.8 | 63.9 | 2.30 | 10.23 | -0.257 |
| 45 | 2250 | 25.90 | 24.3 | 27.8 | 112.0 | 109.0 | 113.0 | 272 | 267 | 286 | -65.0 | -13.8 | -1.5 | 44.8 | 63.9 | 2.21 | 13.79 | -0.245 |
| 50 | 2500 | 23.50 | 19.7 | 28.4 | 110.0 | 102.0 | 116.0 | 269 | 259 | 286 | -49.7 | -11.8 | -0.4 | 45.4 | 63.4 | 2.24 | 12.54 | -0.268 |
| 55 | 2750 | 14.10 | 19.8 | 23.1 | 90.9 | 102.0 | 110.0 | 255 | 261 | 296 | 10.2 | 7.6 | 4.9 | 36.7 | 70.4 | 2.65 | -3.59 | -0.289 |
| 60 | 3000 | 22.30 | 21.6 | 23.8 | 105.0 | 102.0 | 107.0 | 265 | 259 | 271 | -42.0 | -6.7 | 1.1 | 43.5 | 64.9 | 2.32 | 9.53 | -0.254 |

Figure 4-10 shows the particle distribution statistics of D10, D50 (median), and D90, with feedstock values presented by the dashed horizontal lines. At 1,000 g/m$^3$ to 2,500 g/m$^3$ the samples of material not injected have D10 and D50 values greater than the feedstock. D90 values increase as loaded concentration values increase from 750 g/m$^3$

to 2,000 g/m$^3$. At the loaded dust concentration of 2,750 g/m$^3$ D10, D50, and D90 values drop below the feedstock's measured values.

The material not injected from intended PPC concentration of from 750 g/m3 to 2,000 g/m$^3$ show a shift to slightly larger particle sizes for D10 and D50 values. D90 values for the material not injected trends up with an increasing loaded dust concentration. This could indicate some air classification is accruing.

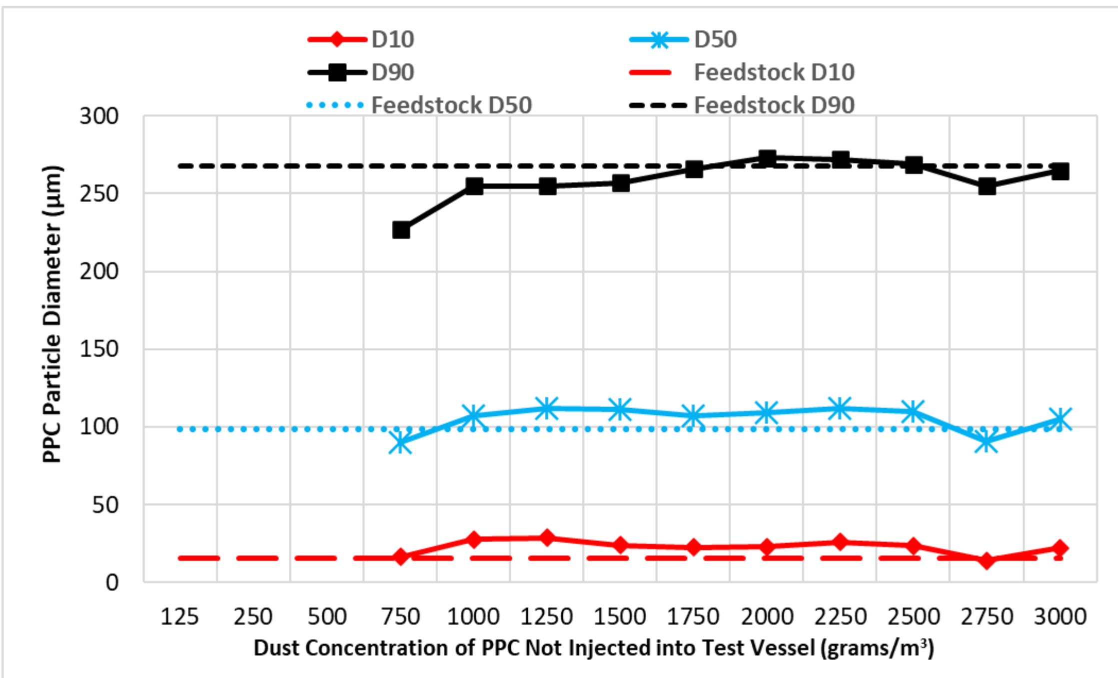


Figure 4-10 Dust Particle Size Statistics of PPC Remaining in Loading Chamber for Intended Dust Concentrations Tested along with Feedstock (Dashed Lines are Feedstock Values)

Figure 4-11 plots cumulative particle size distribution along with the original PPC feedstock particle diameters. For illustrative purposes only five intended dust concentrations are plotted to decrease crowding. The general trend is consistent for all dust concentrations. Figure 4-11 shows the lowest concentration to the farthest left effectively equal to the feedstock distribution. The high-density intended dust concentration had the most change in particle size. Each subsequent increase in intended dust concentration from 1,500 g/m$^3$ shows no significant change. Generally, dust sampled from the loading chamber contain fewer particles from 10 micron to 100 micron.

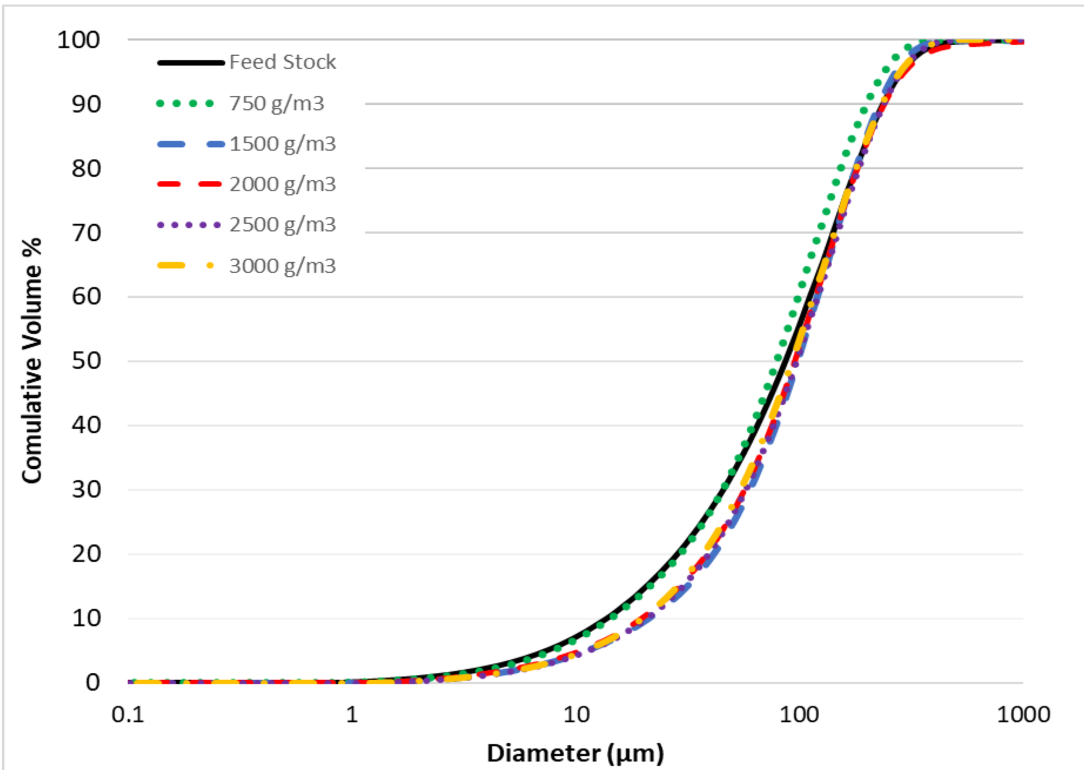


Figure 4-11 Cumulative Particle Size Distribution of PPC Feedstock and Dust not Injected at Different Concentrations

Figure 4-12 shows less dust particles below 40 micron compared to the feedstock plot in black. No material retained in the loading chamber had measurable quantities of material smaller than 1 micron. The retained materials all had higher volume percentage of dust particles around 100 microns than the PPC feedstock. The right side of all plotted trends do not show a significant change in the volume percentage of larger particles greater than 200 micron. It is the largest PPC dust particles that are remaining in the loading chamber. Material less than 100 micron are exiting the loading chamber at slightly higher quantities than larger particles.

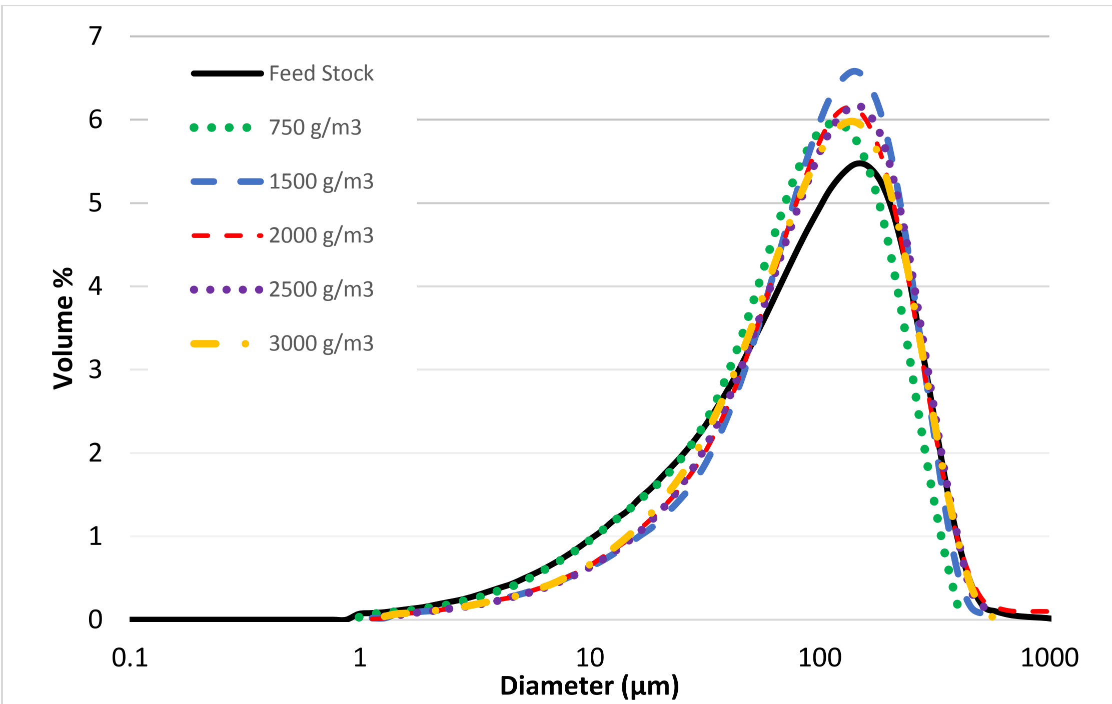


Figure 4-12 Particle Size Distribution of PPC Feedstock and Dust not Injected at Different Intended Concentrations

The mass of PPC dust not injected into the combustion chamber of the 20-L vessel was recorded for each test shot and the data can be seen in Figure 4-13, the mass not injected at lower magnitudes is close to zero. The mass loaded into the loading chamber was mostly injected. At loads above 30 grams of PPC dust the quantity of material not injected is greater than zero and repeatability between test series has high variability. There are four instances where 9 or more grams of loaded PPC dust was collected from the loading chamber after injection, thus not injected.

In Figure 4-14 the data is plotted based on the percentage of recovered PPC mass not injected to loaded mass. The lower concentrations tested with masses below 25 grams had two percent or less of the powder not injected and recovered from the loading chamber. At test quantities of 25 grams and greater the amount of PPC not injected has higher variability. In four instances 20 percent or more of the loaded material was not injected into the combustion chamber. The four instances discussed are directly correlated to the four test shots missing 9 grams or more plotted in Figure 4-13.

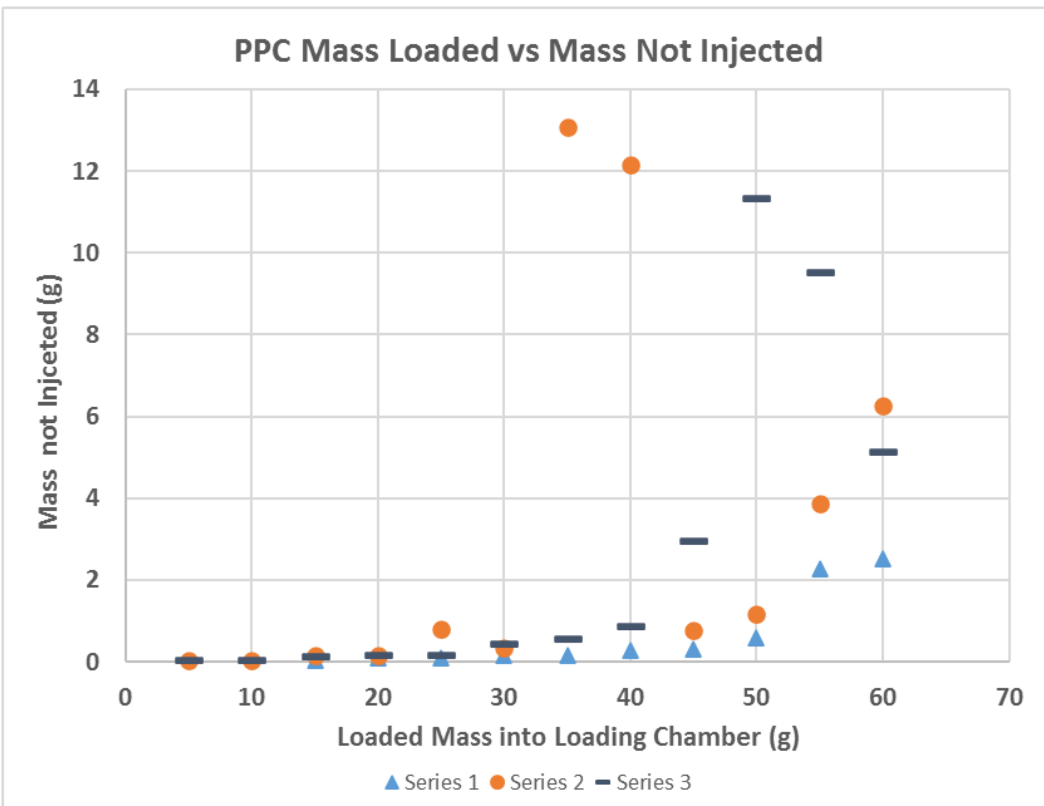


Figure 4-13. Mass of PPC Dust Not Injected into Combustion Chamber

The PPC dust mass remaining in the loading chamber will result in explosive characteristic testing data conducted on lower mass and concentrations than expected based on loaded mass quantities.  In some instances a loaded mass of 40 grams  or more will actually be evaluating the explosive characteristics of  a PPC mass of 10 grams less.

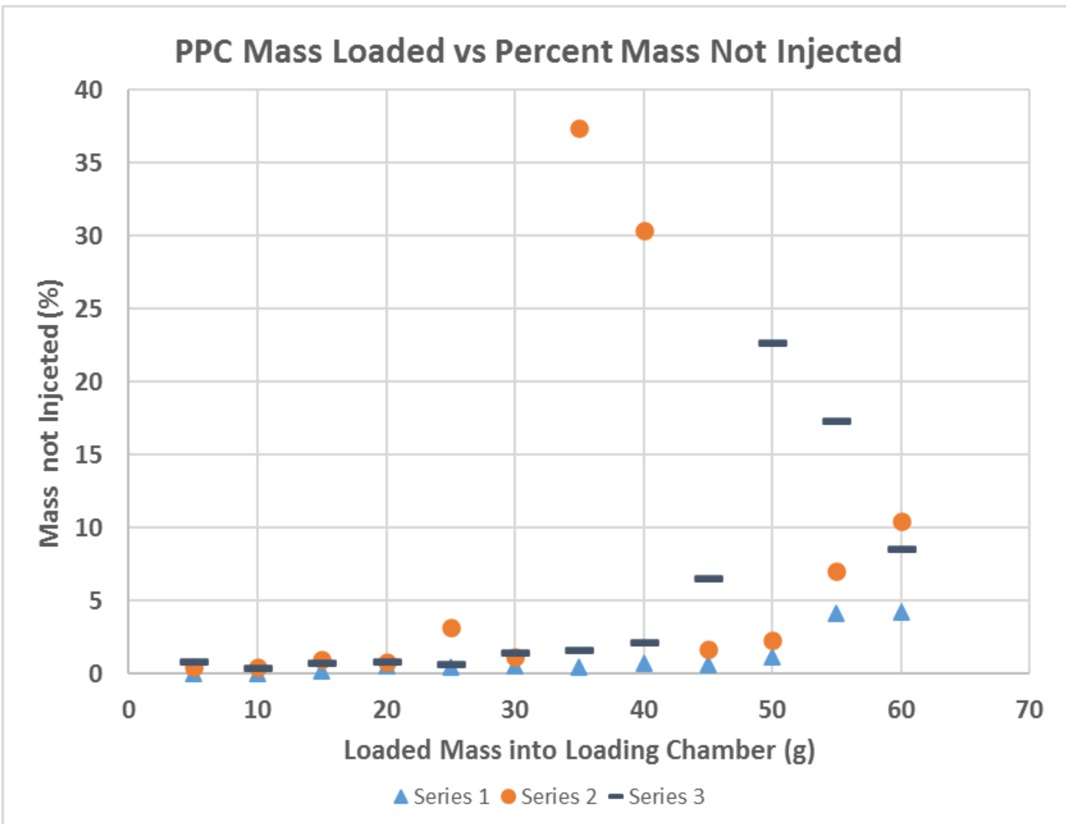


Figure 4-14. Percentage of Mass Not Injected into Combustion Chamber

**4.3.2. Objective 3 Findings.**   Particle size and distribution of dust not injected contains less fines than feedstock material.  Large dust concentrations have a higher volume percentage of particles approximately 100 microns in size compared to low dust concentrations.  The D10, D50, and D90 values of the dust not injected are higher than the original PPC feedstock. There is evidence of air classification occurring where larger particles are not injected into the explosive chamber at the same rate as smaller particles. A summary for objective 3 can be seen in Table 4-9.

Table 4-9. Summary of Objective 3

| | |
|---|---|
| **Objective** | |
| 3 | Quantify dust mass, particle size and distribution that is not injected into the combustion chamber and stays behind in loading chamber. |
| **Hypotheses** | |
| | The particle size and distribution of dust not injected is different than the feedstock's distribution. Large dust concentrations will have a particle distribution with higher percentage of large particles compared to low dust concentrations. |
| **Conclusion** | |
| | Particle size and distribution of dust not injected contains less fines below 40 micron than feedstock material. Large dust concentrations have a higher D10, D50, and D90 values compared to low dust concentrations. The dust loaded does not all get injected into the combustion chamber. Mass of PPC not injected is variable at higher concentrations. |

### 4.4. OBJECTIVE 4: IDENTIFY IF TIGHT PARTICLE DISTRIBUTION AFFECTS EXPLOSION PEAK PRESSURE AND PRESSURE TRENDS VS DUST CONCENTRATION AND REMOVES THE SECONDARY PEAK VALUES AT HIGH DUST CONCENTRATIONS

Testing of 2 different narrow dust concentrations was conducted to see if the particle size affects the peak pressure, pressure vs concentration trends, and mitigates the secondary pressure peak. Testing samples with a narrow particle size distribution will show if only a wide distribution is correlated with the secondary peak and pressure variability. A narrow particle size distribution should have less material that can segregate out under air flow.

The coal dust was sieved and sorted by size so narrow size distributions could be tested in the Siwek 20 L apparatus per ASTM E1226. Dust concentrations from 1500 g/m$^3$ to 3000 g/m$^3$ were evaluated. Table 4-10 lists the different masses of dust evaluated and their equivalent dust concentrations. Testing consisted of 7 tests per dust concentration. A minimum of 42 test shots in the Siwek 20L apparatus.

Table 4-10. Coal Dust Mass and Concentration Evaluated with Narrow Particle Size Distributions

| Coal Dust Mass (g) | 30 | 35 | 40 | 45 | 50 | 55 | 60 |
|---|---|---|---|---|---|---|---|
| Coal Dust Concentration (g/m$^3$) | 1500 | 1750 | 2000 | 2250 | 2500 | 2750 | 3000 |

**4.4.1. Sieve Divided Test Samples and Results.** Two sieve sizes, as shown in Table 4-11, were utilized to sort and segregate coal dust to create test samples with tighter particle size distributions compared to the original feedstock. The mesh size of 100 had a retained particle size of 150 to 300 micron. The mesh size of 200- had a retained particle size of 75 micron and smaller. ASTM E1226 can be tested with as-received dust or 80 percent 75 micron and smaller. USBM testing was conducted with PPC dust 80 percent 75 micron and smaller. PPC feedstock evaluated within this dissertation is roughly 40 percent 75 micron and smaller.

Table 4-11. Mesh Size with Equivalent Particle Size to be Tested

| Mesh size | 100 | 200- |
|---|---|---|
| Particle size | 300-150 microns | 75 microns and smaller |

Figure 4-15 plots cumulative particle size distribution for the two sieve mesh sizes along with the original PPC feedstock particle diameters. The 200- mesh is plotted in red. The 100-mesh size is plotted in blue. The as received feedstock is plotted in black. 95 percent of the 200- mesh material is at or below 75 micron size. 91 percent of the 100 mesh sieved material is equal to or greater than 100 micron. The steep slopes in the plotted data indicate a narrow particle size distribution. The 200+ mesh plot has a slight rise between 10 and 100 micron. The small quantity of smaller than targeted PPC dust particles could be due to finer material passing through previous tighter sieves or it could indicate some comminution occurred during the sieving process.

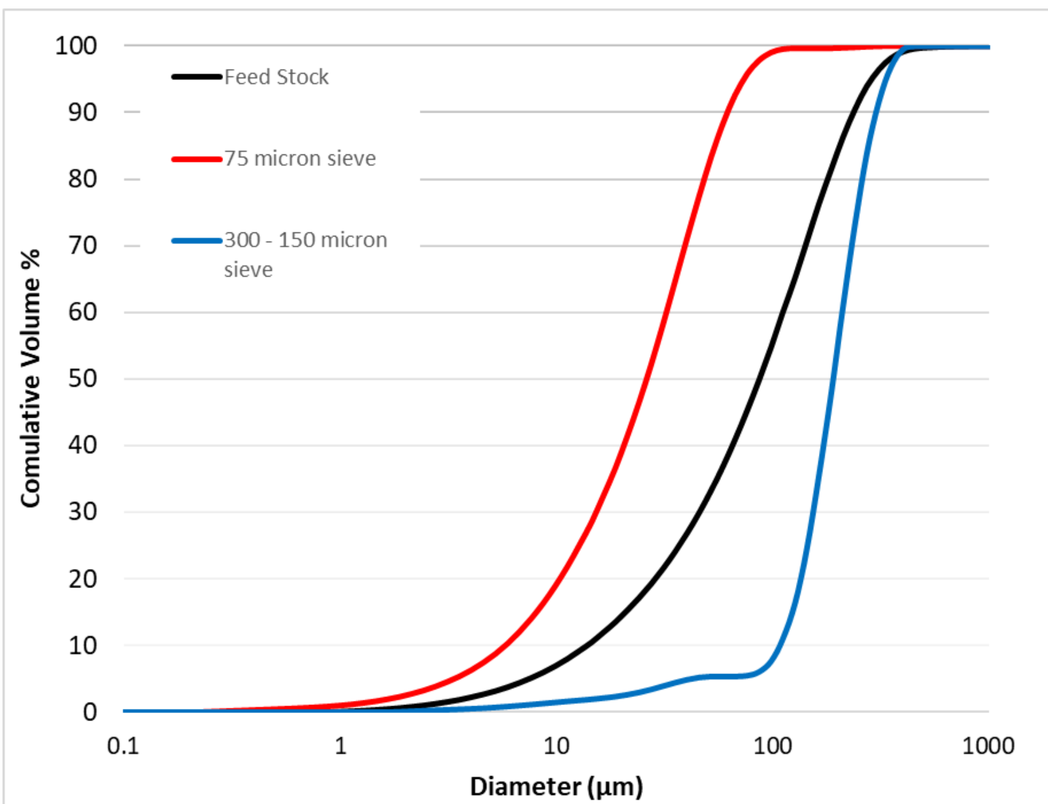


Figure 4-15. Cumulative Particle Size Distribution of as Received Feedstock Coal Dust and Coal Dust Retained by Sieves of Mesh Size 100 and 200-

Figure 4-16 plots particle size distribution for the two sieve mesh sizes along with the original PPC feedstock particle diameters. Again the 200- mesh is plotted in red, the 100 mesh size is plotted in blue, and the original feedstock is plotted in black. Both sieved samples have a narrower distribution than the feed stock. The sieved samples do not have a hard cut off. There is some off sized material in the sieved samples. Some material larger than 75 micron is present in the 200- mesh that should have an upper particle size of 75 micron. The 100 mesh has some material about 75 micron in size.

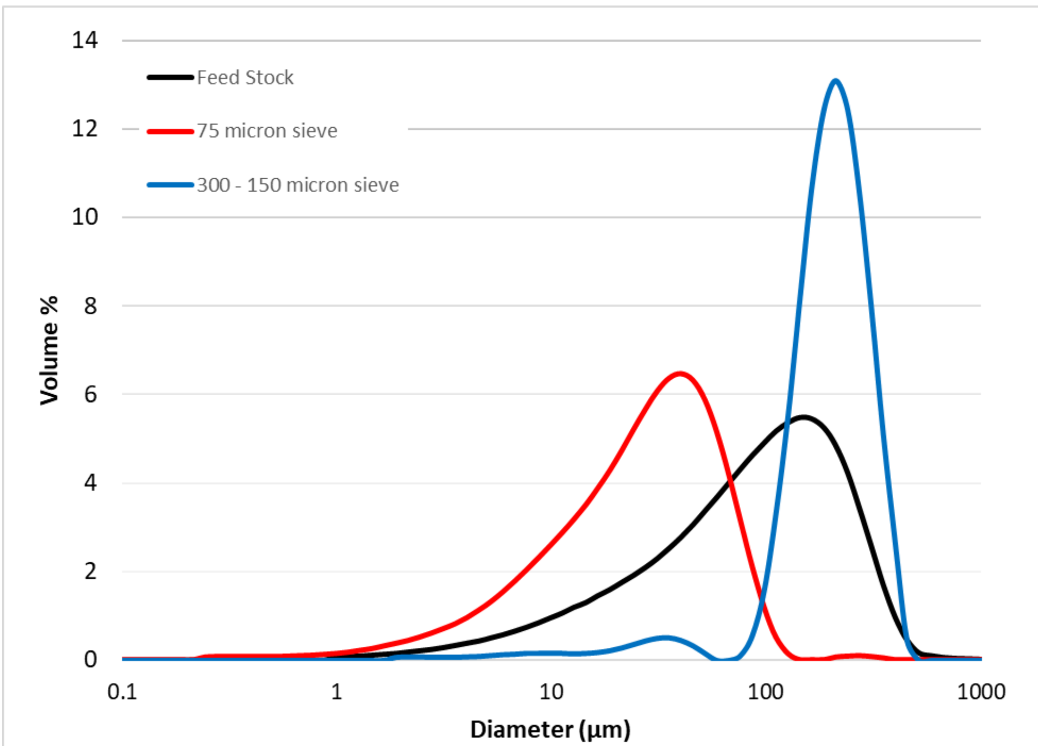


Figure 4-16. Particle Size Distribution of PPC Feedstock and Sieved Test Samples

Dust concentrations between 1150 and 300 g/m$^3$ were evaluated in the Siwek 20L sphere. Each of the sieved samples were evaluated at concentrations shown in Table 4-10. The combustible dust testing was repeated a total of 3 times for each unique combination of sieved sample and dust concentration. The explosive pressure results of the testing can be seen in Figure 4-17. The as received feedstock is plotted with green diamonds with a trend line in black. The 75 micron material is shown with red circles and a red trend line. The 150 -300 micron coal dust is plotted with blue triangles and a blue trend line.

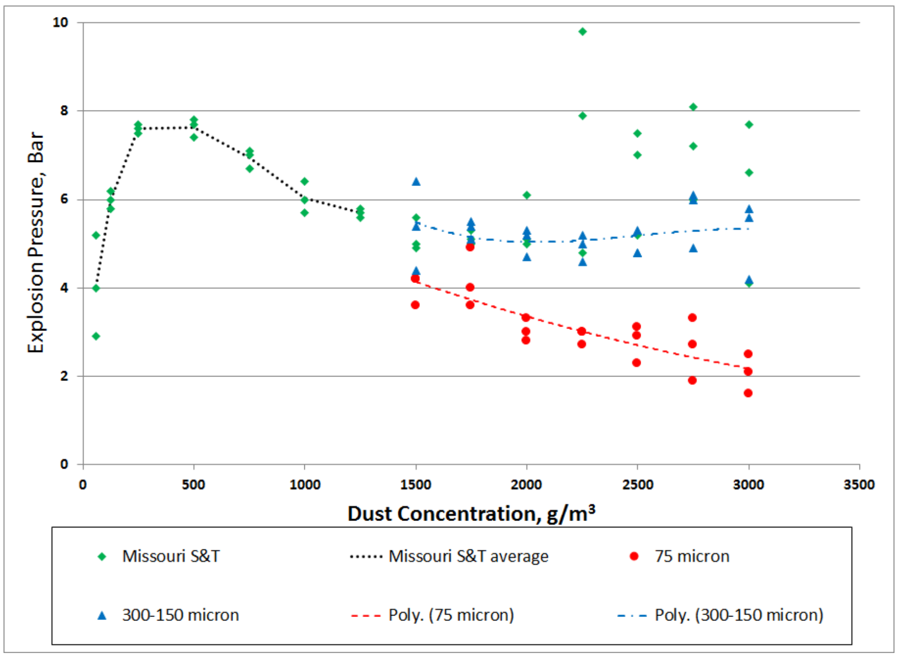


Figure 4-17. Dust Explosion Pressure ($P_{ex}$) Data for as Received PPC Feedstock (Green Diamonds), 75 Micron PPC (Red Circles), 150-300 Micron PPC (Blue Triangles)

All recorded explosion pressures for dust of 150-300 micron are higher than 75 micron PPC tests. Typically, finer dusts react more energetically and produce higher explosion pressures [6]. The recorded test data indicates an inverse tendency. The 75 micron material trends constantly with decreasing explosion pressure as dust concentration increases. PPC dust of 150-300 micron does not follow the same trend and appears to flat-line or slightly increase depending on the type of trend line calculated. It should be noted that the explosive pressure data points for each screened dust size overlap at the dust concentrations of 1,500 and 1,750 g/m$^3$. Though the plotted trend lines are discrete and don't overlap the data points do overlap and become indefinite. Further testing is needed to see at what concentration the different screened tight dust distributions truly converge or become distinct trends.

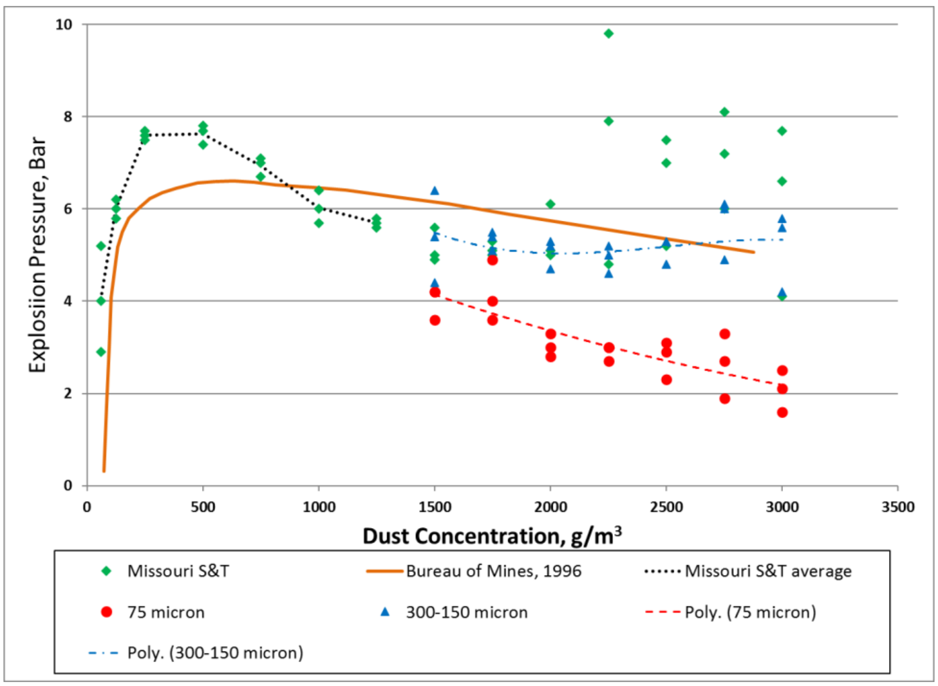


Figure 4-18 Dust Explosion Pressure ($P_{ex}$) Data for as Received PPC Feedstock (Green Diamonds), 75 Micron PPC (Red Circles), 150-300 Micron PPC (Blue Triangles), United States Bureau of Mines [16] Trend (Orange)

In Figure 4-18 a plot of data from the Bureau of Mines is overlaid with the data presented in Figure 4-17. In magnitude, the data and fitted trend line for 150-300 micron PPC dust is close to the USBM published data. The 150-300 micron PPC dust trend line crosses the USBM published data and thus does not have the same slope. The 75 micron

PPC dust has lower explosion pressures than the USBM data. The slope of the trend line for the 75 micron PPC dust and the USBM data appear to be very similar. The USBM data was collected by testing PPC dust described as 80% minus 75 µm [16]. Compared to the initial testing shown in green both sets of screened dust; do not show the secondary peak pressure, have lower explosive pressures (Pe), and have lower variability.

**4.4.2. Objective 4 Findings.** Tight particle size distribution of PPC reduces combustible dust testing peak pressure variability. Different tight particle size distributions of PPC have different reaction pressures and trends. The tight particle size distribution with the smallest particles, 75 micron and smaller, generated lower explosive pressures than larger particle sizes of 150 to 300 micron. This is opposite of what is typically expected with combustible dust where finer dusts react with a higher $K_{st}$ and explosive pressure. Combustibility testing of the tight particle size distribution PPC did not generate the secondary peak pressure witnessed during initial testing. A synopsis of objective 4 can be seen in Table 4-12.

Table 4-12. Summary of Objective 4

| | |
|---|---|
| **Objective** | |
| 4 | Identify if tight particle size distribution correlates to explosion peak pressure and pressure trends vs dust concentration. |
| **Hypotheses** | |
| | A narrow dust size distribution will decrease test output variability. The narrow dust size distribution will not generate the second peak pressure at high concentration levels seen with the as received PPC feedstock. |
| **Findings** | |
| | Tight particle size distribution of PPC reduces combustible dust testing peak pressures, pressure variability, and removed the secondary peak seen during initial testing. |

# 5. CONCLUSIONS

## 5.1. CONDUCTED RESEARCH CONCLUSIONS

The research presented within this dissertation covers testing conducted to investigate the source of a secondary peak pressure for higher concentrations of Pulverized Pittsburg Coal (PPC) dust. Four Objectives were developed to investigate potential sources of the secondary peak pressure and related test output variability. Each Objective in Table 5-1 was directly related to a hypothesis that needed to be evaluated.

Table 5-1. Review of Objectives

| | **Objectives** |
|---|---|
| 1 | Identify Peak Pressure and dust concentration that creates peak pressure between 250 and 500 g/m$^3$. |
| 2 | Quantify dust particle size and distribution that is injected into the combustion chamber. |
| 3 | Quantify dust mass, particle size and distribution that is not injected into the combustion chamber and stays behind in loading chamber. |
| 4 | Identify if tight particle distribution correlates to explosion peak pressure and pressure trends vs dust concentration. |

Objective 1 is related to the hypothesis that a higher $P_{max}$ existed between the dust concentrations of 250 and 500 g/m$^3$ initially evaluated by the author. Testing conducted presented data proving that the peak pressure $P_{max}$ was between 250 and 500 g/m$^3$. The new $P_{max}$ of 7.8 bar was not significantly greater than the value of 7.6 bar revealed during initial testing. Though the hypothesis was correct it did not fully explain the pressure reading of 11 bar at 1,125 g/m$^3$. The higher frequency testing conducted at 1 gram increments validated the standard 20-L operating procedure which recommends a frequency of 5 gram increments [28].

Objective 2 is associated to an operational assumption that the dust loaded within the loading chamber of the Siwek 20L apparatus is the same size and particle distribution of the dust injected into the combustion chamber.  The Author hypothesized that the dust particle size and distribution of dust injected was different than the feedstock's characteristics.  Testing indicated the hypothesis was valid with secondary comminution occurred during the injection and dispersion of the samples into the Siwek 20L L apparatus.

All dust concentrations tested had D10, D50, D90, and D(3,2) values lower than the PPC feedstock.  Lower dust concentrations underwent a greater change than higher dust concentrations, likely due to the equivalent energy used to disperse the dust.  Lower dust concentrations had D10, D50, D90, and D(3,2) values 75% to 50% smaller than the feedstock.  This change in dust characteristics could result in an unknown and unquantified bias.

Testing could not discern how and why secondary comminution was occurring. There are several factors that would have to be studied to quantify how much comminution occurs for each factor and if the factors are independent.  Comminution is dependent on material physical characteristics.  Coal has a lot of jointing and can easily fracture.  Comminution can occur from powder particle to particle and vessel structure interactions during injection and dispersion.  Vessel structures include the rebound nozzle, the isolation valve, and vessel walls.  One can speculate that the rebound nozzle which forces the dust particles to ricochet and change directions may be a significant source of comminution.  The energy available to conduct the work necessary for the secondary comminution is constant.   The pressure differential between the loading and combustion chamber is always the same before injection. If one assumes that pressure differential creates one unit of energy, then as powder mass increases the energy per gram decreases. The work available to each dust particle decreases as the dust concentration increases.

Objective 3 was established to examine if air classification is occurring during dust injection and distribution thus shifting the dust size distribution. It was hypothesized that larger particles were not injected consistently and were more prone to fall out of suspension when air flows from the loading chamber to the explosive testing chamber. Particle size and distribution of PPC dust not injected contains less fines than feedstock material. The D10, D50, and D90 values of the PPC dust not injected are higher than the feedstock. There is evidence supporting the hypothesis of air classification occurring.

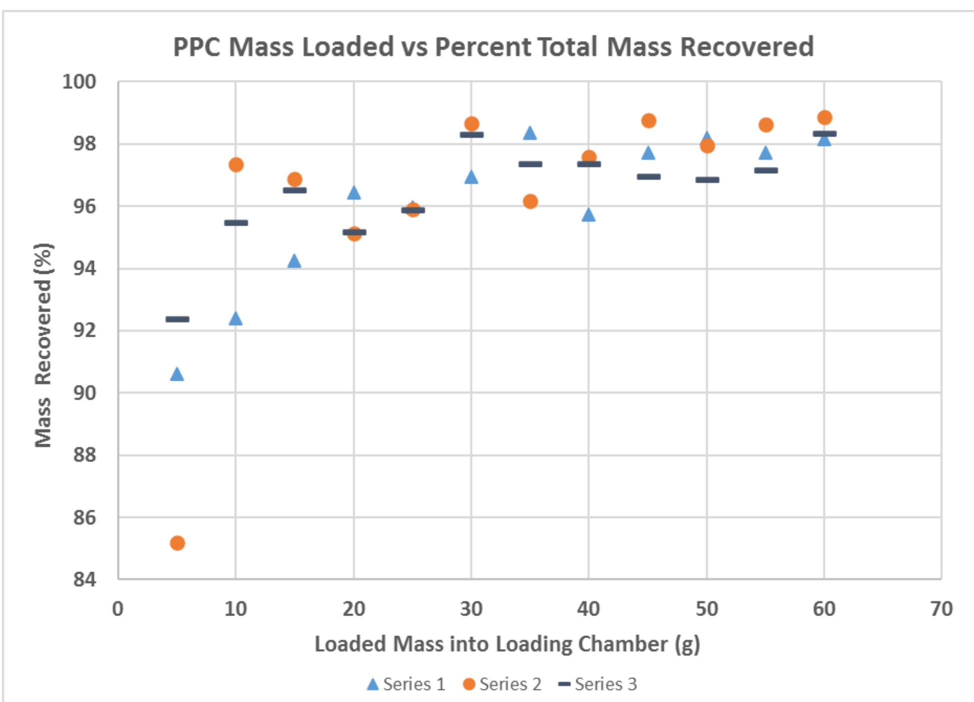


Figure 5-1. Total Percentage of PPC Mass Recovered

Figure 5-1 shows the total percentage PPC mass recovered for each test shot. The mass injected from Objective 2 and the mass not injected from Objective 3 are added together and then divided by the initial loaded mass to calculate the percentage of mass recovered. Only one test recovered less than 90 percent of loaded mass. A majority of test shots recovered 96 percent or more of the initially loaded mass of PPC. The high level of recovered material helps support the validity of the testing conducted in Objectives 2 and 3. Smaller masses are more sensitive to the quantity of dust lost when viewed as a percent recovered. Since the test apparatus is a sealed system it is speculated that the unaccounted quantity of dust was packed into exhaust ports and the upper gas seals of the combustion chamber.

Objective 4 was established to test the hypothesis that a narrow dust size distribution will decrease test output variability. The author hypothesized a narrow dust size distribution would not generate the second peak pressure at high concentration levels as seen with the PPC feedstock. Test evaluation data indicated different particle size distributions of PPC had different reaction pressures and trends. The tight particle size distribution with the smallest particles, 75 micron and smaller, generated lower explosive pressures than larger particle sizes of 150 to 300 micron. Combustibility testing of the tight particle size distribution PPC did not generate the secondary peak pressure witnessed during initial testing and reduces peak pressure and variability.

Overall it has been documented that the mass and particle size of PPC dust injected into the combustion chamber of the 20-L apparatus is not the same as the dust loaded into the loading chamber. Dusts with narrow particle size distributions combust with lower peak pressure variability at high dust concentrations. Different size particles distributions generate distinct pressure trends at higher concentrations.

## 5.2. FUTURE WORK

There is significant work beyond the scope of this dissertation. Topics related to repeatability, impacts to other dusty materials, influence of different testing apparatus are just a few. Recommended future work questions include;

- Do other Siwek 20L apparatus interact with PPC dust in a similar manner?
- Do different combustible dust testing apparatus interact with PPC dust in a similar manner?
- Do other coal dusts react the same within the same Siwek 20L apparatus?
- Do other combustible dusts respond similarly within a Siwek 20L apparatus?
- Can the Siwek 20L apparatus be modified physically or operationally to minimize air classification and ensure total mass of dust loaded is evaluated?
- What is the impact of the unquantified error due to the changes to PPC dust morphology tested within a Siwek 20L apparatus?
- Can computer models of energetic dust reactions be modified to address and simulate secondary comminution and air classification that occurs within a Siwek 20L apparatus?

Does secondary comminution and air classification occur in real world dust explosions and if so what impact does it have on safety calculations, mitigation methodology, and simulations.

# REFERENCES


[1] J. Miller, J. Shafler, E. R. Mulligan, Phillip, K. Perry and C. Johnson, "Explosive Dust Test Vessel Comparison using Pulverized Pittsburgh Coal," *Journal of Archives of Mining Sciences*, vol. 3, no. 63, pp. 713-726, 2018.

[2] J. Miller, P. Mulligan and C. Johnson, "Explosive Dust Characteristics Evaluation of Pulverized Pittsburg Coal using ASTM E1226-12a," in *Proceedings of the 2018 Spring Technical Meeting of the Eastern States Section of the Combustion Institute*, State Collage, PA, 2018.

[3] J. Miller, P. Mulligan and C. Johnson, "Comminution of Pulverized Pittsburgh Coal during ASTM E1226-12A Dust Combustibility Testing," *Powder Technology*, vol. 375, pp. 28-32, 2020.

[4] H. B. Humphrey, "Historical Summary of Coal-Mine Explosions in the United States, 1810-1958," United States Government Printing Office, Washington D.C., 1960.

[5] NIOSH, "Coal Mine Disasters: 1839 to Present," 7 August 2017. [Online]. Available: https://www.cdc.gov/niosh/mining/statistics/content/coaldisasters.html.

[6] R. Eckhoff, Dust Explosions in the Process Industries (3rd Edition), Gulf Professional Publishing, 2003.

[7] OSHA, "Publication 3674: OSHA's Precautions for Firefighter to Prevent Dust Explosions Quick Card," Occupational Safety and Health Administration, Washington, D.C., 2013.

[8] H. Verakis and J. Nagy, "A Brief History of Dust Explosions," in *Industrial Dust Explosions*, West Conshohocken, PA, ASTM International, 1987, pp. 342-350.

[9] G. Rice, "Explosibility of Coal Dust, Bulletin 20," Washington Government Printing Office, Washington D.C., 1911.

[10] J. A. Breslin, "One hundred years of federal mining safety and health research," U.S. Department of Health and Human Services, Public Health Service, Centers for Disease Control and Prevention, National Institute for Occupational Safety and Health, Pittsburgh, PA, 2010.

[11] K. Cashdollar and K. Chatrathi, "Minimum Explosible Dust Concentration Measured in 20-L and 1-m3 Chambers," *Combustion Science and Technology,* vol. 87, pp. 157-171, 1993.

[12] K. Cashdollar, "Overview of Dust Explosibilty Characteristics," vol. 13, pp. 183-199, 2000.

[13] ASTM, "A Century of Progress," 1998. [Online]. Available: https://www.astm.org/ABOUT/history_book.html. [Accessed 30 August 2017].

[14] ASTM E1226-12a, West Conshohoken, PA: ASTM International, 2012.

[15] NFPA 654, "Standard for the Prevention of Fire and Dust Explosions from the Manufacturing, Processing, and Handling of Combustible Particulate Solids," National Fire Protection Association, 2017.

[16] Cashdollar, "Coal dust explosibility," *Journal Loss Prevention in the Process Industries,* vol. 9, pp. 183-199, 1996.

[17] J. Going, K. Chatrathi and K. Cashdollar, "Flammabiltiy limit measurements for dusts in 20-L and 1-m3 vessels," *Journal of Loss and Prevention in the Process Industries, 13,* pp. 209-219, 2000.

[18] K. Cashdollar and M. Hertzberg, "20-l explosibility test chamber for dusts and gases," *Review of Scientific Instruments*, pp. Vol. 56, No. 596, 1985.

[19] S. J. Tewalt, L. F. Ruppert, L. J. Bragg, R. W. Carlton and D. K. Brezinski, "Chapter C - A Digital Resource Model of the Upper Pennsylvanian Pittsburgh Coal Bed, Monongahela Group, Northern Appalachian Basin Coal Region. U.S. Geological Survey Professional Paper 1625–C," 2001. [Online]. Available: https://pubs.usgs.gov/pp/p1625c/.

[20] K. Cashdollar, M. Sapko, M. Hertzberg and E. Weiss, "Laboratory and Mine Dust Explosion Research at the Bureau of Mines," in *Industrial Dust Explosions*, Wst Conshohocken, PA, ASTM International, 1987, pp. 107-123.

[21] C. K. Man and M. L. Harris, "Participation of large particles in coal dust explosions," *Journal of Loss Prevention in the Process Industries 27,* pp. 49-54, 2014.

[22] F. Woskoboenko, "Explosibility of Victorian Brown Coal Dust," *Fuel,* vol. Vol. 67, no. No. *, August 1988.

[23] M. Mittal, "Study of Explosibility Data of Coal Dust for Designing Explosion Safety Measures," *International Journal of Advanced Engineering Technology,* pp. pp. 82-91, July-Sept 2013.

[24] OSHA, "OSHA Law & Regulations," 2017. [Online]. Available: https://www.osha.gov/law-regs.html. [Accessed 8 2017].

[25] OSHA, "Combustible Dust National Emphasis Program, CPL 03-00-008," Occupational Safety and Health Administration, 2008.

[26] OSHA, "Combustible Dust in the Wood Products Industry," Occupational Safety and Health Administration (OSHA), 2009.

[27] NFPA, "List of NFPA codes & standards," August 2017. [Online]. Available: http://www.nfpa.org/codes-and-standards/all-codes-and-standards/list-of-codes-and-standards. [Accessed 8 August 2017].

[28] KuhnerAG, "20L Apparatus Manual, KSEP 7.0," Kuhner AG, Birsfelden, Switzerland, 2011.

[29] Adolf Kuhner AG, "Manual CaRo 15," Birsfelden, Switzerland, 2015.

[30] Adolf Kuhner AG, "Final Report Calibration-Round-Robin CaRo15," Birsfelden, Switzerland, 2016.

[31] ASTM D197-87, West Conshohocken, PA: ASTM International, 2012.

[32] Horiba Scientific, "A Guidebook to Particle Size Analysis," Horiba Instruments, INC, Irvine, CA, 2019.

[33] A. Tascon, "Influence of particle size distribution skewness on dust explosibility," *Powder Technology,* vol. 338, pp. 438-445, 2018.

[34] S. J. Blott and K. Pye, "GRADISTAT: a grain size distribution and statistics package for the analysis of unconsolidated sediments," *Earth Surface Processes and Landforms,* vol. 26, pp. 1237-1248, 2001.

# VITA

Jacob Lee Miller graduated from the Missouri University of Science and Technology with a doctoral degree in Explosives Engineering in December 2021. His education and professional preparation focused on ballistic impacts, explosive breaching, dust explosions, manufacturing process design and prototyping. He has been responsible for developing, testing, manufacturing and evaluating the performance of energetic systems in both his doctoral and master's research, as well as in his work with Y-12 National Security Complex.

Some of Mr. Miller's most recent projects included explosibility characterization of combustible dusts, explosive breaching of hardened concrete structures, explosively formed projectiles from bulk charges, shockwave interaction with a cylindrical target, and impulse loading from a buried explosive. He published and presented his research with the Combustion Institute 2018 ESSCI Spring Technical Meeting and the 2019 EFOG Nuclear & Facility Safety Subgroup Conference.

Jacob Miller has also earned three masters degrees and one bachelor degree. The degrees were in Mining Engineering, Explosives Engineering, Manufacturing Engineering and Mechanical Engineering respectively.